2020

# Epigenetic alterations at synaptic plasticity genes in a genetically heterogeneous rat model of neuropsychiatric disorders

Doan M. On
*Virginia Commonwealth University*

**Epigenetic alterations at synaptic plasticity genes in a genetically heterogeneous rat model of neuropsychiatric disorders**

A thesis submitted in partial fulfillment of the requirements for the degree of Master of Science in Physiology & Biophysics at Virginia Commonwealth University

By
Doan Minh On
B.S. Biology, University of Virginia, 2010
M.S. Biochemistry & Biophysics, University of North Carolina at Chapel Hill, 2014

Director: Javier González-Maeso
Associate Professor
Department of Physiology & Biophysics

Virginia Commonwealth University
Richmond, Virginia
March 2020

## ACKNOWLEDGEMENTS

I extend my utmost gratitude to my parents, Tai On and Phuoc Nguyen, for their seemingly boundless supply of motivation and support. I will always cherish the revitalizing feeling of their love when, after an unexpectedly long day in lab, a frozen home-cooked meal awaited. I also extend my gratitude to my sister Jade and brother Bao for being there in ways that parents could not. Together we complement and together we make a formidable team.

To Dr. Aznar Kleijn and Tina Østerbøg, I extend my warmth and appreciation, for without their expertise and steady hand in generating and analyzing data, this study would have not been possible.

To each member of the González-Maeso lab, I offer my fond regards. Their sterling personalities and talents created a *sui generis* atmosphere, as warm as their hearts and as brilliant as their ideas. Getting to work with them, to learn from them, and to know them, both in lab and out, has been a singular delight, and I treasure our shared memories.

Finally, to my advisor Dr. González-Maeso, I convey my deepest, most heartfelt gratitude. I arrived at his doorstep naïve to neuroscience. He attended to my training needs with kindness and compassion throughout my tenure, and even amidst change, he remained a pillar of support. With effort I contributed and with time I learned, emerging humbled by how little we know. At least now I know I can engage with the unknown, better equipped with the tools he helped me realize I have.

## LIST OF PUBLICATIONS & MANUSCRIPTS

1. Østerbøg TB*, On DM*, Oliveras I, Río-Álamos C, Sanchez-Gonzalez A, Tobeña A, González-Maeso J, Fernández-Teruel A, Aznar S. (2019). *denotes co-first author status

   **Metabotropic Glutamate Receptor 2 and Dopamine Receptor 2 Gene Expression Predict Sensorimotor Gating Response in the Genetically Heterogeneous NIH-HS Rat Strain.** *Mol Neurobiol* (2019). https://doi.org/10.1007/s12035-019-01829-w.

2. Hideshima KS, Hojati A, Saunders JM, On DM, de la Fuente Revenga M, Shin JM, Sánchez-González A, Dunn CM, Pais AB, Pais AC, Miles MF, Wolstenholme JT, González-Maeso J. (2018).

   **Role of mGlu2 in the 5-HT2A receptor-dependent antipsychotic activity of clozapine in mice.** *Psychopharmacology* 235, 11: 3149-65.

3. Sierra SS, On DM, …, González-Maeso J.

   **Epigenetic regulation of *Calcrl* in chemotherapy-induced peripheral neuropathy.**
   *(in preparation)*

# TABLE OF CONTENTS

## LIST OF ABBREVIATIONS

| | |
|---|---|
| PPI | Prepulse inhibition of the acoustic startle response |
| ChIP | Chromatin immunoprecipitation |
| qPCR | Quantitative polymerase chain reaction |
| CNS | Central nervous system |
| Grm2 | Metabotropic glutamate receptor subtype 2 |
| Htr1a | 5-Hydroxytryptamine (serotonin) receptor 1A |
| Htr2a | 5-Hydroxytryptamine (serotonin) receptor 2A |
| Drd1 | Dopamine receptor D1 |
| Drd2 | Dopamine receptor D2 |
| Gapdh | Glyceraldehyde 3-phosphate dehydrogenase |
| NMDA | *N*-methyl-D-aspartate |
| PCP | Phencyclidine |
| H3ac | Pan-acetylated histone H3 |
| H3K27me3 | Trimethylation of lysine residue 27 of histone H3 |
| RHA | Roman high avoidance |
| RLA | Roman low avoidance |
| NIH-HS | National Institute of Health Heterogenous Stock |
| gDNA | Genomic DNA |
| HDAC | Histone deacetylase |
| s.e.m. | Standard error of the mean |
| bps | Base pairs |

## ABSTRACT

Sensorimotor gating impairments are observed across a range of neuropsychiatric conditions. The prepulse inhibition of the acoustic startle response (PPI) is a validated measure of sensorimotor gating. Genetic and pharmacological manipulations in rodents have shown PPI is regulated by specific brain monoaminergic systems. Using genetically heterogeneous *NIH-HS* rats, we stratified individuals by %PPI. In low PPI animals, we observed elevated mRNA levels of certain neurotransmitter receptors, including metabotropic glutamate receptor *Grm2*, dopamine receptors *Drd1* and *Drd2*, serotonin receptors *Htr1a* and *Htr2a*, and scaffolding protein *Homer1*, in the frontal cortex (FC) and striatum (STR). We found *Drd2* mRNA levels were significantly increased in the low PPI group in STR. Multinomial regression analysis indicated *Grm2* in FC and *Grm2* and *Drd2* in STR predicted PPI group. Additional studies showed a linear relationship between PPI and *Grm2* in FC and *Drd2* in STR. To explore possible epigenetic regulation of altered gene transcription, we adapted chromatin immunoprecipitation (ChIP) for novel application in frozen brain tissue. We evaluated abundance of acetylated histone H3 (H3ac) and trimethylation of lysine residue 27 of histone H3 (H3K27me3) at regions upstream of gene transcription start sites. No differences in levels of H3ac or H3K27me3 were observed. Studies assessing abundance of other histone modifications are warranted. These efforts may offer insight on how epigenetic modification leads to altered transcription of synaptic plasticity genes regulating sensorimotor gating observed in neuropsychiatric conditions.


## CHAPTER 1: INTRODUCTION

At the 7th World Congress of Psychiatric Genetics, those dedicated to understanding molecular mechanisms of the mind were met with a puzzle. In psychotic disorders like schizophrenia, there was a high degree of discordance in twin and family studies (DeLisi et al., 2000, 2000; Kendler and Diehl, 1993). If genes determine phenotype, what could be playing a role in psychiatric traits not predicted by rules of Mendelian inheritance? Faced with these facts, genes it seemed were more dispositional than dispositive in disease processes, and conferees

broached the idea of epigenetics to offer some explanation in schizophrenia and other related disorders (Petronis et al., 2000). Toward the turn of the century, the field of epigenetics has emerged to address this puzzle, providing yet more insight into the etiology of human diseases. The polygenic and multifactorial nature of neuropsychiatric disorders underscores the importance of investigations into epigenetic mechanisms which may reconcile the dual influence of genes and environment. This study in *heterogeneous stock* (*HS*) rats aims to characterize patterns of histone modifications at genes regulating sensorimotor gating. Locus-specific alterations in histone modification could provide important insights into epigenetic mechanisms governing transcriptional regulation in neuropsychiatric disorders.

## DEFINITIONS OF EPIGENETICS

Epigenetics is not a novel paradigm yet it aims to revise the central dogma of molecular biology. The term 'epigenetics' was borrowed from the field of embryology, used to refer to the developmental theory of epigenesis (Waddington, 1942). Epigenesis proposed the notion that organisms could ultimately trace their origins to a progenitor cell, entirely undifferentiated (Holliday, 1994). The competing theory of preformation on the other hand staked the claim that within germ cells lay tiny, prototypical embryos. With time, technology, and the discovery of genes, notion of preformation was debunked, as molecular biology firmly demonstrated that DNA and its molecular intermediaries were determinative in the developmental fate of cells, and thus of the organism. In the second half of the twentieth century, as scientific minds sought to connect genes to disease aided by yet finer DNA biotechnologies, the field of genetics came to the fore, while epigenetics, as originally conceptualized, was relegated to the realm of niche research.

In its broadest operational definition, epigenetics can be defined as various phenotypic interpretations of a single genome sequence. In other words, epigenetics describes a phenomenon, literally "above the genes," that allows for the panoply of cellular phenotypes from one original blueprint within a single cell without changing individual A, T, G, or G nucleotides.

What are the molecular mediators that determine cell fate, that allow certain genes to be expressed and others repressed?

Several areas of epigenetics, including DNA methylation, histone posttranslational modification (PTM), and microRNAs, can serve to regulate gene expression (Cedar and Bergman, 2009; Grewal and Moazed, 2003; Henikoff and Shilatifard, 2011; Strahl and Allis, 2000). Perhaps the best-known epigenetic alteration is DNA methylation that occur within CpG islands. DNA methylation is thought to be involved in the spatiotemporal control of gene expression during development. Its misregulation is commonly observed in cancer, where promoter hypermethylation silences tumor suppressor genes to promote malignant transformation. CpG island methylation plays an important role in transcriptional regulation, and it is commonly altered during malignant transformation (Baylin and Jones, 2011; Dawson and Kouzarides, 2012; Sproul and Meehan, 2013). The functional relevance of these regional alterations in methylation are yet to be fully deciphered, but it is interesting to note that they have challenged the general dogma that DNA methylation invariably equates with transcriptional silencing. Another growing subfield of epigenetics includes microRNA-mediated gene downregulation. Just twenty-two nucleotides in length, these small RNA species negatively regulate target gene expression via a posttranscriptional mechanism called RNAi or RNA interference. RNAi is naturally triggered in the presence of double-stranded RNA of viruses and constitutes a defense mechanism in eukaryotes. microRNAs exert their effect of gene silencing when they bind cognate mRNA via sequence complementarity, thus targeting the mRNA for enzymatic degradation.

### CHROMATIN STRUCTURE AND FUNCTION

Chromatin reflects the strategy that nature evolved to fit the genome within the nucleus, some 6 microns in diameter (Figure 1). Its most basic unit is the nucleosome particle, around which a length of 147 DNA base-pairs (bp) are coiled. The nucleosome core is octameric, consisting of two copies of each of the four core histone proteins (H2A, H2B, H3 and H4). The octamer assembles when a tetramer of two H3 and H4 complexes with two H2A/H2B dimers

(Andrews and Luger, 2011; Luger et al., 1997), and this assembly in turn binds approximately three billion DNA base pairs around about 30 million nucleosomes in humans. This effectively reduces DNA length from 2 meters to the so-called ‘beads on a string’ model, with each bead representing one nucleosome, as first depicted by electron microscopists. Additional higher-order folding ultimately results in the textbook X-shaped structure commonly known as a chromosome, and when viewed as a whole after Giemsa staining, distinct bands can be discerned, chromatin can be loosely or tightly structured, termed euchromatin or heterochromatin, respectively.

Beyond a role in DNA compaction, chromatin actively participates in the regulation of DNA replication, repair, and transcription. Studies have observed a range of altered transcriptional outcomes when chromatin state is altered locally, such as reorganization of nucleosome density, or globally, as seen in gene silencing via heterochromatinization. Each nucleosome particle contains eight histone monomers that have solvent-exposed N-terminal tails subject to covalent post-translational modifications (PTMs) by enzymatic complexes. There is a growing number of histone PTMs, including methylation, acetylation, phosphorylation, ubiquitination, ADP ribosylation, SUMOylation, crotonylation, citrullination, among others.

Several mechanisms have been described to explain how histone PTMs can influence gene expression. The charge neutralization model posits that certain PTMs result in structural changes to the DNA-histone complex. Electrostatic repulsions between negatively charged PTMs, such as acetylation ($CH_3COO^-$) or phosphorylation ($OPO_3^{3-}$) on adjacent nucleosomes, leads to an open conformation of chromatin (Bannister and Kouzarides, 2011). This model however fails to explain histone methylation which can be associated with transcriptional activation or repression depending on the amino acid residue modified. In the signaling network model, the presence of histone PTMs signals for recruitment of additional effector proteins (Schreiber and Bernstein, 2002), such as chromatin modifiers, nucleosome remodelers, and/or transcription factors that may subsequently act on the chromatin template. Last, the histone code hypothesis proposes that certain patterns of histone PTMs are interpreted by effectors, either in

sequence or in tandem, to specify unique outcomes (Strahl and Allis, 2000). Efforts to decipher the 'histone code' and their effect on gene transcription in healthy and pathological contexts have provided some clues (Kouzarides, 2007; Tan et al., 2011).

Many lysine residues on histone tails, including H3K4, H3K9, H3K27, H3K36, H3K79, and H4K20, can be methylated. Methylation of H3K4, H3K36, and H3K79 residues are associated with active transcription in euchromatic gene regions, while H3K9, H3K27, and H4K20 methylation is associated with silenced genes within heterochromatin (Barski et al., 2007). Lysine residues moreover may be mono-, di-, or trimethylated, and interesting patterns for the valence of histone lysine methylation have been observed to localize within certain upstream regulatory gene regions. For instance, H3K4me3 spans the transcriptional start site (TSS) of active genes , H3K4me1 is associated with active enhancers (Heintzman et al., 2009), and H3K4me2 seems to demarcate regions of transcription factor binding. Likewise, H3K9me1 may be seen at transcriptionally active genes, while H3K9me3 and H3K27me3 are associated with gene repression (Barski et al., 2007). What is clear is that histone PTMs are numerous and complex and may dynamically convey environmental cues (*i.e.*, drugs of abuse, early life stress) to genes, serving to tune their expression resulting in phenotypes beyond what inheritance alone would predict.

**MODELING NEUROPSYCHIATRIC CONDITIONS IN RODENTS**

Neuropsychiatric disorders encompass neurological, neurodevelopmental, and psychiatric conditions. Together, they are leading causes of disability in the United States, accounting for 19% of all years of life lost to disability and premature mortality (The US Burden of Disease Collaborators et al., 2018). In any given year, an estimated 18% of US adults suffer from mental illness, according to the Center for Behavioral Health Statistics and Quality. Over 50% of people in middle- and high-income countries will at some point in their lives come to be afflicted as well. The worldwide incidence of those suffering from mental disorders is estimated at 450 million people, according to the World Health Organization. Neuropsychiatric conditions are of

consequence beyond the afflicted individuals. Between 2011 and 2030, the loss of economic output from neuropsychiatric conditions is estimated at 16 trillion USD, higher than that of cancer, respiratory diseases, and diabetes (Trautmann et al., 2016).

In the 1980s, linkage studies among family, twin, and adopted cohorts in humans lent credence to the notion that genes contribute to psychiatric phenotypes (Gottesman and Carey, 1983; Kendler and Robinette, 1983; Kessler, 1980; McInnis et al., 1999; Stine et al., 1995). Research aimed at identifying genetic factors that predispose individuals to neuropsychiatric conditions has been steady since. Biotechnological advances in molecular biology and bioinformatics have further strengthened this idea by enabling association studies in yet larger cohorts, revealing candidate gene and gene regions. The advent of next generation sequencing technology has unveiled genetic factors that have eluded detection by candidate approaches. However, identified hundreds or even thousands of genes each contribute less than one percent to overall risk of specific disorder (Gratten et al., 2014). Expression profiling in human cerebral cortex across five major neuropsychiatric conditions (autism, schizophrenia, bipolar disorder, depression, and alcoholism) found patterns of differentially expressed genes unique to each and shared across conditions (Gandal et al., 2018). Despite larger data sets and higher-throughput screens, mounting studies recapitulate many of the same major findings of earlier works: the genetic architecture of major psychiatric disorders is highly polygenic and shares substantial etiological overlap. In general, promising study findings have not translated, as psychiatric conditions range widely in cause, course, and severity.

One of the first examples linking genes to addiction was in selective breeding studies of rat strains exhibiting differential susceptibility to morphine (Nichols and Hsiao, 1967). Numerous studies since have identified genes contributing to addiction of other substances, such as ethanol (Gilpin et al., 2008) and methamphetamine (Wheeler et al., 2009), as well as other in psychiatric conditions, like mood and anxiety disorders and schizophrenia. Studies in the inbred rat strains Roman high avoidance (RHA) and Roman low avoidance (RLA) for instance have been useful to

reveal strain-specific behavioral traits, including coping mechanisms in response to stress, measures of impulsivity, and PPI. Notably, RHA rats exhibited a higher degree of impulsivity and susceptibility to substance abuse, as well as diminished performance on tasks of attention, spatial learning, and sensorimotor gating (Oliveras et al., 2015). In addition, RHA rats display an enhanced dopaminergic response to drugs of abuse and aversive stimuli within the frontal cortex and striatum, followed by elevated cortical serotonin levels (Giorgi et al., 2003). These molecular and behavioral observations suggested the RHA strain may serve as a putative model for impaired PPI. Compared to inbred rat strains, outbred rodent models like the *NIH-HS* rat strain have also been used. The genetically heterogenous *NIH-HS* colony was generated at the National Institutes of Health from eight inbred founder strains (Hansen & Spuhler, 1984). Since their origination in 1984, colonies have been maintained by a pseudorandom breeding scheme aimed at maximizing genetic variation. *HS* animals have been employed to fine-map complex traits relevant to conditions ranging from diabetes and heart disease to anxiety and addiction. This feature makes the *NIH-HS* rat model especially useful for investigations of the genetic and neurobiological correlates of complex psychiatric traits, like deficits in PPI response.

### LINKING EPIGENETICS WITH MOLECULAR PSYCHIATRY

Owing the failure to translate promising study findings to therapeutic application, current models of neuropsychiatric conditions now emphasize the interaction of environmental and social factors across life course, as well as a component of genes. Given the disappointment surrounding genome association studies for some neuropsychiatric disorders, focus has turned to mechanisms which can mediate changes in gene expression independent of changes to DNA sequence, like posttranslational modification of histones. Numerous histone modifications are likely involved in regulation of the acquisition and maintenance of neuropathological states, with histone acetylation and methylation as the most characterized to date. Changes in histone acetylation have offered clues into how the environment can induce broad transcriptomic changes by altering the epigenetic landscape via histone PTMs (Borrelli et al., 2008). There is now ample

evidence that some measure of the environment plays a role in the progression of neuropsychiatric disease (Volkow et al., 2019). Because of the strong influence of external risk factors on the likelihood that an individual develops a neuropsychiatric condition, it may be that epigenetic mechanisms regulate the early prodromal period and consequently leading to a pathophysiological state. Ample studies demonstrate that cocaine regulates histone acetylation in rodents (Renthal et al., 2009; Rogge and Wood, 2013). Interestingly, long-term cocaine exposure resulted in Hdac5-dependent behavioral sensitization to subsequent doses and to stressors, while acute exposure did not (Renthal et al., 2007). This suggested a homeostatic balance of histone acetylation regulates saliency of environmental stimuli, disruption of which may be involved in the transition from an acute adaptive response to a chronic psychiatric illness like drug addiction.

Studies have also investigated epigenetic regulation of stress resilience by histone acetylation in rodents. One study showed that rats selectively bred on the basis of their high novelty-induced motor activity (high-responders) were subjected to environmental stress and their preference for sucrose solution was measured (Hollis et al., 2011). High-responders post-stress exhibited less sucrose preference compared to low-responders, a change that was mirrored in levels of acetylated histone H3 and H2B within the hippocampus.

Histone methylation also dynamically alters chromatin state underlying pathophysiological responses to stress, as well as to psychotropic drug treatments, in rodents. Another study found that social or isolation stress resulted in widespread alterations in methylation of H3K27 levels at the upstream regulatory regions across a wide swath of genes, among which are involved in transcriptional regulation themselves (Wilkinson et al., 2009). In the rat/mouse hippocampus following chronic social defeat stress, BDNF levels are diminished concurrent with repressive histone modifications. Notably, antidepressant treatment was found to upregulate *BDNF* expression via histone acetylation (Tsankova et al., 2006). However in the nucleus accumbens, social stress induces a state of hyperacetylation of histone H3 associated with decreased Hdac2,

which can be restored by HDAC inhibitors to promote stress resilience (Covington et al., 2009). Interestingly, learning and memory has been shown to be regulated in part by H3K4 methylation, dysregulation of which is associated with impaired cognition and intellectual disability (Collins et al., 2019). Though studies looking at histone modifications in depressed human post-mortem samples are scant, a study of the prefrontal cortex has reported altered levels of histone methylation (H3K4me3 and H3K27me3) in promoter regions of *BDNF* (Chen et al., 2011). Together, these findings suggest that epigenetic processes regulate neurophysiological processes like synaptic plasticity in rodents via gene transcription and may be leveraged for therapeutic intervention in human disease.

### PREPULSE INHIBITION: A BEHAVIORAL MODEL OF SENSORIMOTOR GATING

A number of neuropsychiatric disorders are linked by impairments in sensorimotor gating, an important pre-attentive process of the central nervous system (CNS). Sensorimotor gating deficits can be quantified by measuring the prepulse inhibition of the acoustic startle reflex. Prepulse inhibition, or PPI, is the suppression of the startle reflex when the intense startling stimulus is immediately preceded by a barely detectable prestimulus (Graham, 1975). Ample studies support PPI as an operational measure of sensorimotor gating (Swerdlow et al., 2016).

Deficiencies in sensorimotor gating can cause profound dysfunction in everyday activities across a range of diagnostic domains, depending on the nature of the intrusive stimulus whether motor, sensory, or cognitive. Evolutionarily, this inhibitory gating process is thought to safeguard the integrity of information salient to survive within a complex environment. In healthy individuals, sensorimotor gating allows for appropriate behaviors by suppressing or ‘gating’ irrelevant exteroceptive or interoceptive stimuli. These so-called ‘gating disorders’ share the criterion of a deficiency in inhibitory process within the CNS (Braff et al., 1978, 2001; Mcghie and Chapman, 1961) and can bridge developmental, psychiatric, and neurological diagnostic domains (Table 1). The observation of faulty sensorimotor gating across this wide range underscores the primacy of

behavioral inhibition, attention, and selective information processing in generating healthy behavioral responses.

**TABLE 1. EXAMPLES OF 'GATING' DISORDERS**

| Disorder | Deficient in gating of… | Resulting in… | Reference |
|---|---|---|---|
| Schizophrenia | Thoughts, sensory stimuli | Hallucinations, impaired cognition, psychosis | (Braff et al., 1978) |
| Autism spectrum | Thoughts, speech, actions | Stereotypy, obsessions | (McAlonan, 2002) |
| Obsessive-compulsive disorder | Repetitive, intrusive thoughts | Ritualistic behaviors | (Ahmari et al., 2012; Swerdlow et al., 1993) |
| Tourette's syndrome | Thoughts, speech, movements | Involuntary motor or phonic outbursts | (Castellanos et al., 1996; Zebardast et al., 2013) |
| Huntington's disease | Unintentional movements | Adventitious movements, chorea | (Swerdlow et al., 1995; Valls-Solé et al., 2004) |

**MONOAMINE NEUROTRANSMITTER RECEPTORS IN SENSORIMOTOR GATING**

The PPI paradigm has also proven useful for probing the neurobiological substrates underlying sensorimotor gating. The neuroanatomy involved in PPI has been localized within the basal forebrain in rodent studies. Lesions of the dorsomedial striatum (Baldan Ramsey et al., 2011) or infusion of dopamine into the nucleus accumbens impair PPI response (Swerdlow, 1994). Neural connections that link the limbic cortex with the striatum particularly by the ventral striato-pallidal circuitry are believed to modulate the response (Kodsi & Swerdlow, 1996). Based on previous studies and on the relevance of the monoamine and glutamate neurotransmitter systems as drug targets in neuropsychiatric 'gating' disorders, we focused on genes encoding for serotonin receptor subtype 1a *Htr1a*, serotonin receptor subtype 2a *Htr2a* (Farid, 2000), metabotropic glutamate receptor subtype 2 *Grm2* (Grauer & Marquis, 1999), dopamine receptor type 2 *Drd2* (Swerdlow et al., 1990), and the postsynaptic scaffolding protein *Homer1*. RLA and RHA strains exhibit differences in impulsivity, as measured by the 5-choice serial reaction time task. RHA animals display enhanced impulsive behavior concomitant with increased serotonin in

the striatum and nucleus accumbens, as compared to RLA animals (Moreno et al., 2010). Within the frontal cortex of RHA and RLA strains, a pattern of differential binding of highly specific radioligands for monoamine receptors Htr1a, Htr2a, and Grm2 has been shown, as well as a correlation between Htr2a binding and measures of impulsivity (Klein et al., 2014).

The receptor pharmacology of certain compounds can also be used to experimentally induce sensorimotor gating deficits. For instance, disruption of PPI can result from drugs that facilitate dopaminergic activity, such apomorphine (Geyer and Swerdlow, 1998; Martinez et al., 2000; Swerdlow and Geyer, 1993), amphetamine, or cocaine. Using near-identical stimulus parameters between species, the PPI paradigm can also be leveraged to predict efficacy of antipsychotic compounds (Swerdlow and Geyer, 1998), and alleviation of apomorphine-mediated PPI impairment is correlated with clinical antipsychotic drugs in a potency- and *Drd2* dopamine receptor affinity-dependent manner (Swerdlow et al., 2006). Serotonin receptors have also been shown to mediate the PPI response. Rats given an intracortical infusion of DOI, a Htr2a receptor agonist, have increased measures of impulsivity and exhibit pronounced PPI deficits (Sipes and Geyer, 1995; Wischhof et al., 2011). Moreover, blockade of Htr2a-mediated intracellular signaling attenuates impulsivity-like behaviors induced by cocaine, amphetamine, or MK-801 (O'Neill et al., 1999). In addition to involvement of brain dopamine and serotonin systems, glutamatergic neurotransmitter systems like the N-methyl-D-aspartate (NMDA) receptor have a role in the PPI response and sensorimotor gating. Studies using NMDA antagonists, such as phencyclidine, ketamine, and MK-801 (Fletcher et al., 2011; Mansbach and Geyer, 1991; Martinez et al., 2000), expanded on the PPI paradigm. Frontline pharmacological agents used in patients with schizophrenia, such as the typical antipsychotic haloperidol and the atypical antipsychotic clozapine, can restore in rats PPI deficits induced by apomorpine (Swerdlow, 1994). Together these studies suggest the involvement of monoamine neurotransmitter receptors in psychiatric 'gating' disorders. Indeed, there is considerable target overlap, given drugs that modulate monoamine neurotransmitter system are used to treat psychotic, anxiety, and mood disorders.

While the clinical reality of using the PPI paradigm to predict antipsychotic efficacy is limited for those who need it, the involvement of forebrain monoamine and glutamate systems is clear.

### STUDYING EPIGENETICS BY CHROMATIN IMMUNOPRECIPITATION ASSAY OF HISTONE PTMS

Chromatin immunoprecipitation (ChIP) is a useful biochemical assay in the study of epigenetic processes, especially in assessing distribution and relative abundance of target histone modifications and binding or occupancy of transcription factors and multi-protein complexes on DNA. Histone modifications can work in concert with DNA methylation to regulate cellular structure, function, and environmental exposure (*i.e.*, drugs of abuse, early life stressors) (Cedar and Bergman, 2009). More than 130 unique histone modifications have been described to date, and chromatin immunoprecipitation allows for the exploration of their associations with the regulatory regions of target genes and other DNA/chromatin-associated proteins across the genome (Strahl and Allis, 2000). Many variations of ChIP have been developed in the 30 years since its earliest version came into use, which makes it challenging for users to integrate the procedure into their research programs. Furthermore, differences between various protocols can confound efforts to increase reproducibility across studies. Hence, before setting out to test our hypothesis, we conducted pilot studies of ChIP parameters, including conditions of sonication, chromatin solubilization, and Protein A/G bead substrate.

The steps of a basic ChIP protocol are depicted in Figure 5. Briefly, dissected tissue is treated with fixative to crosslink molecules *in situ*. Following lysis, crosslinked chromatin is released from nuclei and solubilized. Chromatin is subsequently sheared by sonication to produce fragments amenable to immunoprecipitation by antibodies selective for histone modifications. The chromatin-antibody complex—and the DNA associated to the histone modification—is retrieved by addition of beads and serially washed to eliminate non-specific interactions. Immunoprecipitated DNA is eluted, proteins are digested, and then crosslinks reversed. Purified DNA is isolated by phenol-chloroform extraction and ethanol precipitation. Finally, abundance of immunoprecipitated DNA is quantified by qPCR assay and normalized to input.

# CHAPTER 2: MATERIALS AND METHODS

### ANIMALS

A total of 39 male rats from 30 different litters of the *National Institute of Health-Heterogenous Stock* (*NIH-HS*) strain were used. This strain was derived in 2004 from an outcross breeding strategy of eight inbred strains (*MR/N*, *WN/N*, *WKY/N*, *M520/N*, *F344/N*, *ACI/N*, *BN/SSN*, and *BUF/N*) (Hansen and Spuhler, 1984). A permanent colony of *NIH-HS* rats is maintained at the Medical Psychology Unit, Department of Psychiatry and Forensic Medicine, School of Medicine, Autonomous University of Barcelona). Rats used for experiments were screened by prepulse inhibition testing session, as described (Oliveras et al., 2015). Rats were housed in same-sex pairs under standard conditions (12 hr: 12 hr light/dark cycle; 22 ± 2˚C; 50-70% humidity; food and water *ad libitum*) in Macrolon cages (50 × 25 × 14 cm). Rats were approximately four months old of age (mass: 320-400 g) at time of experimentation.

### PREPULSE INHIBITION (PPI) OF ACOUSTIC STARTLE REFLEX

To segregate *NIH-HS* rats into low and high experimental groups, animals were individually assessed for PPI behavior in a sound-attenuated box (SR-Lab Startle Response System, San Diego Instruments, San Diego, USA) (Oliveras et al., 2015; Rio-Alamos et al., 2019). Within each box, rats were placed in a cylinder atop a platform rigged to a piezoelectric sensor to detect the acoustic startle response at 65, 70, 75, and 80 dB. Startle response was measured throughout the whole session. The PPI behavioral assessment was performed during the light cycle. Each startle session included the following:

1) Habituation: 5 min

2) Background noise of 55 dB + 10 single-pulses of 105 dB for 40 ms.

3) 10 × of each block below (set of 6 randomized trials [a-c])

    A) 1 × 55 dB background

    B) 1 × [55 dB background + 105 dB pulse for 40 ms] for baseline response

C) 1 × [55 dB background + 65/70/75/80 dB prepulse for 20 ms + 105 dB pulse for 40 ms]

4) 5 × [55 dB background + pulse of 105 dB for 40 ms]

Startle response was measured throughout the whole session. Only measurements of startle response after 3B and 3C sessions were used to calculate the PPI response, as a percentage for each of four prepulse intensities. The arithmetic mean of each prepulse intensity was calculated and is represented by *% $PPI_{total}$* (hereinafter: PPI response).

$$\%\ PPI = 100 - \frac{\text{mean response of 3C trials}}{\text{mean response of 3B trials}} \times 100$$

$$\%\ PPI_{total} = \frac{\Sigma\ (\%\ PPI\ )}{4}$$

**MRNA EXTRACTION AND PURIFICATION**

Four weeks after segregation of *NIH-HS* rats by PPI response, animals were humanely euthanized per institutional guidelines. Separate tissues comprising frontal cortex and striatum coordinates were harvested, whereupon one hemisphere (~100 mg) was flash frozen in liquid nitrogen for RNA isolation (see directly below) and the other (~100 mg) crosslinked in formaldehyde for chromatin immunoprecipitation assays (see farther below). Tissues were stored at −80˚C in nitrogen phase until analyzed.

RNA was extracted using the NucleoSpin® RNA/Protein kit (Macherey-Nagel; 740933) per manufacturer's protocol. Briefly, tissue was homogenized and lysed in buffer containing 1% β-mercaptoethanol. Genomic DNA (gDNA) was removed from extracted total RNA by on-column digestion with RNase-free DNase I (Ambion; AM1907). RNA concentration was spectrophotometrically quantified by NanoDrop 2000c (Thermo Scientific). Quality was assessed by Bioanalyzer 2100 (Agilent Technologies). Two samples were excluded based on the following criteria: A260/A280 ratio less than 1.8 or RNA integrity number (RIN) value less than 5. RNA was stored at −80˚C until analysis by quantitative polymerase chain reaction (qPCR).

### qPCR Analysis of mRNA Expression

For gene expression analysis, qScript cDNA 5x SuperMix (Quanta; 95048) was used per manufacturer's protocol. In brief, 200 ng purified mRNA were reverse transcribed into complementary DNA (cDNA) (25°C for 5 min; 42°C for 30 min; 85°C for 5 min; and stored at 4°C). cDNA products were diluted 1:4 in RNase/DNase-free water and kept at -20°C until the qPCR assay. Products were assayed in triplicate on a 96-well plate. Each reaction well contained the following components: appropriate primer sets, diluted cDNA, RNase/DNase-free water, and 2x Fast SYBR Green master mix (Applied Biosystems; 4385612). Each plate was run on the QuantStudio 3 Real-Time PCR System (Applied Biosystems; A28567) with optimized thermocycle profiles for each primer set. For sequences of RT-qPCR oligonucleotides, see Table 2.

Gene targets *Grm2*, *Drd1*, *Drd2*, *Htr1a*, *Htr2a*, and *Homer1* used the following thermocycle profile: 10 min at 95°C; 40 cycles of 15 s at 95°C (melt); 30 s at 60°C (anneal & extension). Reference genes *Gapdh* and *Rpl13a* used the following profile: 10 min at 95°C; 40 cycles of 15 s at 95°C (melt); 30 s at 60°C (anneal); 30 s at 72°C (extension), per manufacturer's guidelines (Table 3). RNase/DNase-free water was substituted in place of diluted cDNA as a negative control. cDNA derived from Rat Universal Reference total RNA (Agilent Technologies; 740200) controlled for intraplate variance. Specific and on-target amplification was confirmed by the presence of a single sharp peak by melting curve analysis (Østerbøg TB *et al.*, collaborator's master's thesis entitled "Gene expression profiles associated with sensorimotor gating response in the genetically heterogeneous *NIH-HS* rats" submitted January 28, 2018). Relative gene expression was calculated by the $2^{-\Delta\Delta Ct}$ method (Livak and Schmittgen, 2001), normalizing first to the two reference genes, *Gapdh* and *Rpl13a*, then to experimental controls. Expression levels of housekeeping genes did not differ across groups.

### Western Blotting

We conducted pilot studies using magnetic and polyacrylamide beads due to limited tissue quantity and differences in binding capacity of these protein A/G resin substrates for

immunoprecipitation. Two or five μg anti-H3K27me3 antibody were conjugated to polyacrylamide UltraLink Resin (Thermofisher Scientific; 53132) or magnetic beads (ThermoFisher Scientific; 88802) for 16 hours at 4˚C on an end-over-end rotator. The antibody-bead complex (bound fraction) and the flow-through containing unbound antibody were collected for analysis by Western blot.

Western blot experiments were performed as previously reported in (González-Maeso et al., 2008) with minor modifications. Briefly, samples were denatured in Laemmli sample buffer, resolved by SDS-PAGE, and transferred to nitrocellulose. Membranes were probed with 1:200 dilution of primary antibody (anti-kappa light chain Ab, Novus Biologicals; NBP2-15191) followed by incubation with HRP-conjugated secondary antibody (Amersham Biosciences). Washes were conducted with TBS-T + 0.1% Tween-20. Immunoreactive proteins were visualized with enhanced chemiluminescence (ThermoScientific) on Odyssey infrared imaging system (LI-COR Biosciences) per manufacturer's protocol.

**CHROMATIN CROSSLINKING**

Immediately after harvest of relevant brain tissues by collaborators at the University of Copenhagen, one hemisphere from a single animal was fixed in 1% formaldehyde at RT. After 20 min, crosslinking was quenched by addition of concentrated glycine (Sigma; G8898) to a final concentration of 0.125 M for 5 min at RT. Samples were then centrifuged at 1,500 × g for 5 min at 4°C, and the supernatant containing flocculate masses was aspirated. The pellet containing fixed homogenates were resuspended in 1 mL PBS + 0.1% Protease Inhibitor Cocktail (Sigma; P8340) and transferred to a new tube and centrifuged as before. The supernatant was aspirated, and the pellets were immediately flash frozen and stored at −80°C until the ChIP assay. Fixed and frozen specimens were shipped to Virginia Commonwealth University in dry ice by collaborators.

**OPTIMIZATION OF CHROMATIN SOLUBILIZATION AND FRAGMENTATION**

Ideal conditions for chromatin solubilization and fragmentation were determined to maximize qPCR signal. Tissue was subjected to lysis under conditions of (1) whole cell lysis or (2) hypotonic lysis followed by nuclear lysis. Treatment with SDS lysis buffer generates whole cell lysate, while hypotonic lysis buffer selectively ruptures the cytoplasmic membrane, yielding nuclei which are subsequently subjected to lysis. Approximately 100 mg of frozen and fixed tissues with hippocampal coordinates of *NIH-HS* animals were used to test DNA fragmentation conditions. The cell density of test tissue was similar to tissues used later in ChIP assays. To solubilize crosslinked chromatin, tissue was treated with SDS lysis buffer (50 mM Tris, 10 mM EDTA, 1% SDS), yielding whole cell lysate, or hypotonic lysis buffer (50 mM HEPES-KOH, pH 7.4, 140 mM NaCl, 1 mM EDTA, 10% glycerol, 0.5% IGEPAL CA-630 (Sigma-Aldrich; I-3021), and 0.25% Triton X-100 (Sigma-Aldrich; BP151)), yielding nuclei. Nuclei were rinsed with wash buffer containing 10 mM Tris-Cl, pH 8.1, 200 mM NaCl, 1 mM EDTA, and 0.5 mM EGTA, and then lysed in nuclear lysis buffer (10 mM Tris-Cl, pH 8.1, 100 mM NaCl, 1 mM EDTA, 0.5 mM EGTA, 0.1% deoxycholate (Sigma-Aldrich; D-6750), and 0.5% N-lauroylsarcosine (Sigma-Aldrich; L-9150)).

Chromatin was fragmented with a Q700 sonication system (QSonica; CL-334) with microtip attachment. The duration of sonication was determined, starting with 2 cycles at 10 pulses (1 sec on and 1 sec off) for a total process time of 20 sec per cycle at 8% amplitude and increasing to 10 cycles. Each tube was incubated on ice for at least 90 sec between cycles to prevent premature de-crosslinking or denaturation of antibody epitope. Ten µL of fragmented chromatin was removed after each cycle. After fragmentation of DNA and clarification by high-speed clarification at 16,000 × g for 15 min at 4˚C, 10 µL treated with 2 µL of 10 mg/mL Proteinase K (ThermoFisher; AM2546) at 55˚C for 2 hr followed by 1 µL of 20 mg/mL RNase A (Invitrogen; 12091039) at 37˚C for 1 hr. Samples were incubated at 65˚C for at least 4 hr to reverse crosslinks. DNA was purified by phenol/chloroform/isoamyl alcohol extraction followed by ethanolic

precipitation. Purified samples were resolved electrophoretically on a 1.5% TAE (Tris base, acetic acid, and EDTA, pH 8.3) gel with Orange G loading dye (NEB; B7022S).

**CHROMATIN IMMUNOPRECIPITATION ASSAY**

Chromatin immunoprecipitation was performed as described with minor modification (McCullough et al., 2017). Pellets containing crosslinked histone proteins and DNA (chromatin) were fractionated to selectively lyse the cytoplasm and isolate intact nuclei. Nuclei were resuspended in ice-cold lysis buffer supplemented with Protease Inhibitor Cocktail II (Millipore; 539132) and 100 mM PMSF (Sigma; P7626). Extracted chromatin was sonicated for 7 cycles, as described above. Following clarification by high-speed centrifugation at 16,000 × g for 15 min at 4˚C, 20 µL of the supernatant containing sheared chromatin was collected and stored at 4˚C for input DNA. The remaining extract was prepared for immunoprecipitation with ChIP-grade antibodies specific for rabbit anti-H3K27me3 (2 µg, Millipore; 07-449); rabbit anti-H3ac (5 µg, Millipore; 06-599), or rabbit IgG (5 µg, Millipore; 12-370). Antigen-antibody complexes were retrieved by co-addition of polyacrylamide A/G resin (ThermoFisher Scientific; 53132). After 16 hours, the protein/DNA/resin complexes were collected by gentle centrifugation (1,000 × g for 1 min). To remove non-specific interactions, samples were washed in a series of four ice-cold buffers (1 mL for 5 min at 4˚C on an end-over-end rotator for each): (1) low salt wash buffer (20 mM Tris, pH 8.1, 150 mM NaCl, 2 mM EDTA, 1% Triton X-100, 0.1% SDS), (2) high salt wash buffer (20 mM Tris, pH 8.1, 500 mM NaCl, 2 mM EDTA, 1% Triton X-100, 0.1% SDS), (3) LiCl wash buffer (10 mM Tris, pH 8.1, 1 mM EDTA, 1% IGEPAL CA-630, 250 mM LiCl, 1% sodium deoxycholate), and (4) TE buffer (10 mM Tris, pH 8.5, 1 mM EDTA). Next, immunoprecipitated protein/DNA complexes were eluted from the resin. Immunoprecipitated genomic DNA and input samples were treated with proteinase K, DNase-free RNase A, and de-crosslinked by incubating at 65˚C for at least 4 hr. DNA was purified by phenol/chloroform extraction and precipitated, as described directly below. The precipitated DNA was resuspended in TE buffer and stored at −20˚C until qPCR analysis.

### PRECIPITATION OF IMMUNOPRECIPITATED GDNA FRAGMENTS

Following protein digestion, RNase treatment, and decrosslinking, immunoprecipitated gDNA was purified by phenol/chloroform/isoamyl alcohol (PCI) extraction (ThermoFisher; 15593031) followed by ethanolic precipitation. One volume of PCI was added to the sample and thoroughly vortexed before centrifuging 3 min at 13,000 × g at room temperature. The upper aqueous layer was transferred to a new tube and back-extracted with an equal volume of freshly prepared 1:1 (v/v) chloroform/isoamyl alcohol solution. Following resolution of layers, the upper aqueous layer was transferred to a new tube. Forty-four µL of 3 M sodium acetate (pH 5.2), 2 µL of 20 mg/mL glycogen (Invitrogen; R0561), and 1 mL of 100% ethanol were added. This mixture was thoroughly vortexed and precipitated at −80°C overnight. The DNA was pelleted by high-speed centrifugation (15,000 × g for 20 min at 4°C) and washed twice with 1 mL of 70% ethanol (chilled to −20°C). DNA pellets were dried and resuspended in TE buffer. To visualize sonicated chromatin, DNA was loaded with Orange G dye and resolved on a 1.5% agarose/TBE gel (Voytas, 2000) stained with 0.4 µg/mL ethidium bromide alongside a DNA ladder. The gel was de-stained in TBE buffer, as necessary, and visualized on a UV transilluminator.

### QPCR ANALYSIS OF CHROMATIN IMMUNOPRECIPITATED GENOMIC DNA (CHIP-QPCR)

Genomic abundance of chromatin immunoprecipitated DNA was assessed by qPCR with validated primer sets. Each reaction well contained the following components: 2 µL genomic DNA, 200 nM primers, and 2X PowerUp SYBR® Green Master Mix (ThermoFisher; A25742) and was prepared in quadruplicate in a 384-well microplate. Each plate was run on the QuantStudio 6 Flex Real-Time PCR System (Applied Biosystems; 4485691) with the following thermocycle program: 2 min at 50°C; 2 min at 95°C; 45 cycles of 15 s at 95°C and 1 min at 60°C. All primer sets displayed on-target specificity by melt curve analysis. Melt curve analysis was conducted (5 min of 60 to 95°C at 0.05˚C/s, 15 s at 95°C) to verify on-target genomic amplification. Relative genomic abundance of histone modifications at target genomic loci was expressed as % of input, as based on a previous publication (Kurita et al., 2013). Briefly, Ct values of input DNA were corrected with

respect to the volume removed from the total immunoprecipitation volume. The Ct values corresponding to genomic targets were then calculated utilizing the $2^{-\Delta\Delta Ct}$ method (Livak and Schmittgen, 2001) to obtain % of input values.

Genome sequence for *Rattus norvegicus* were obtained from ENCODE (Davis et al., 2018; ENCODE Project Consortium, 2012). ChIP-qPCR primers were designed for the genes *Grm2*, *Htr1a*, *Htr2a*, *Drd2*, and *Homer1* at three upstream regions, including transcriptional start site (TSS), proximal promoter (up to 1 kb upstream of TSS), and distal promoter (approximately 1.4 kb upstream of TSS). For *Gapdh*, only primers targeting the proximal promoter were designed. For sequences of ChIP-qPCR oligonucleotides, see

Table 4.

**STATISTICAL METHODS**

Statistical analyses were performed with GraphPad Prism 8. Kruskal-Wallis test with *post hoc* Dunn's multiple comparison test was conducted for analyzing the PPI response across the different groups. For the mRNA expression, a D'Agostino & Pearson Omnibus normality test indicated that some data were not normally distributed. Multiple *t* tests with Holm-Šidák's *post hoc* correction was conducted. Outliers were identified and excluded by the ROUT method (Q=1%). A model was constructed by a multinomial logistic regression analysis with PPI response (dependent variable) and mRNA expression (independent variable). Models were constructed independently for each genomic region. Genes with significant contributions to statistical model were subjected to regression analysis for confirmation. Statistical significance of H3ac and H3K27me3 ChIP assays was assessed by Mann-Whitney U tests at promoter region of *Gapdh* or by two-way ANOVA with Šidák's multiple comparison corrections at gene regions of all other genes. The level of significance was chosen at $p = 0.05$. Data are presented as mean ± s.e.m. For detailed statistical analyses in tabular form are presented in the Appendix.

# CHAPTER 3: RESULTS

### SEGREGATION *OF NIH-HS* RATS INTO GROUPS BY PPI RESPONSE

Column analysis was performed for 39 *HS* rats based on individual PPI response, or %PPI. Animals were subsequently segregated into three groups (Figure 2 and Table 5). For PPI response, rats scoring in the first quartile (n=10) and last quartile (n=10) were placed into low PPI and high PPI groups, respectively; rats in the interquartile range (n = 19) were placed in a medium PPI group. Two-way ANOVA of PPI responses of these groups showed a significant difference in the %PPI of each group for each of four prepulse stimulus intensities (65, 70, 75, 80 dB), as well as for total % PPI. After Dunn's multiple comparisons test, significant differences between the low PPI and high PPI groups remained (Table 6).

### INCREASED MRNA EXPRESSION IN LOW PPI GROUP

When comparing the relative mRNA expression between the extreme PPI groups for frontal cortex (Figure 3A), a statistically significant increase in *Grm2*, *Drd2*, *Htr1a*, and *Homer1* was observed in the low PPI group compared to the high PPI group. There were no differences in *Drd1* and *Htr2a* mRNA levels. After correcting for multiple comparisons, differences were no longer significant. In striatum (Figure 3B), a statistically significant increase in relative mRNA levels of *Drd2*, *Htr1a*, and *Htr2a* was observed in the low PPI group, as compared to the high PPI group. There were no differences in mRNA levels of *Grm2*, *Drd1*, and *Homer1*. Following correction for multiple testing, only *Drd2* maintained significance.

### REGRESSION ANALYSIS OF GENE EXPRESSION & PPI RESPONSE

We conducted a multinomial logistic regression analysis of all genes, PPI groups, and brain regions to determine the extent to which mRNA expression may pattern PPI response. The resulting model indicated that mRNA expression predicted the clustering of *HS* animals into their corresponding PPI group (

Table 7). In testing mRNA expression of individual genes for goodness-of-fit, we found that *Grm2* in the frontal cortex and *Drd2* and *Grm2* in the striatum contributed significantly to the

model. In focusing on these genes, we subsequently sought to confirm correlation between mRNA expression and PPI response in a linear regression analysis. There was a statistically significant linear relationship between PPI and *Grm2* expression levels in the frontal cortex ($F_{(1,32)} = 9.5$; $R_2 = 0.23$; $p = 0.0043$; slope = − 0.051, std. error = 0.017) (Figure 4A) and *Drd2* expression in the striatum ($F_{(1,33)} = 5.2$; $R_2 = 0.14$; $p = 0.0286$, slope = − 1.4, std. error = 0.60) (Figure 4B). However, no statistically significant linear relationship was seen between PPI and *Grm2* expression in the striatum ($F_{(1,36)} = 2.3$; $R_2 = 0.06$; $p = 0.1391$).

#### ADAPTATION OF CHROMATIN IMMUNOPRECIPITATION ASSAY

Due to technical variability of the ChIP assay, pilot studies were undertaken to determine optimal conditions in rat brain tissue. We first set out to determine best technical conditions of the ChIP protocol in our hands, focusing on a few key steps of the assay which we have previously experienced as critical for success. The first of these studies looked into the most variable step of the ChIP protocol: sonication by ultrasound treatment. Sonication serves two main purposes: first in facilitating solubilization and second in shearing of chromatin into fragments tractable for immunoprecipitation and more reliable mapping of the target histone modification by qPCR. To determine how many cycles were necessary with our sonication setup, after successive sonication cycles small sample amounts were removed for analysis. Visualization of agarose-resolved DNA fragments showed a cycle-dependent shift in the average electrophoretic mobility of fragments, with successive cycles producing a smaller average fragment size over a narrower range (Figure 6A). Based on reported guidelines, we determined that six sonication cycles were sufficient to yield the appropriate range of fragment sizes amenable for immunoprecipitation.

The next preliminary study looked into buffer conditions into which chromatin is solubilized and then sonicated. To liberate crosslinked protein-DNA adducts, similar amounts of brain tissue were subjected to lysis by either whole cell or nuclear lysis after selective removal of cellular contents (*e.g.*, plasma membrane components, cytoskeleton, cytoplasmic proteins and nucleic acids) under hypotonic conditions (hereinafter: nuclear lysis). Although both methods achieved

sufficient solubilization post-sonication, conditions of whole cell lysis yielded a higher apparent amount of soluble DNA over nuclear lysis (Figure 6B). Despite the difference in efficiency of solubilization, we chose to sonicate under nuclear lysis conditions because only the DNA-protein interactions within the nuclear compartment were of relevance in this study.

We next compared the binding capacities of polyacrylamide resin and magnetic beads which are commonly used substrates to capture antibody-antigen complexes from solution in immunoprecipitation assays. To this end, either 2 or 5 μg anti-H3K27me3 ChIP-grade antibody were conjugated to identical volumes of polyacrylamide resin or magnetic beads overnight. The flow-through, containing unbound antibody, and the bound fraction, containing the antibody-substrate complex, were then subjected to polyacrylamide gel electrophoresis under denaturing conditions (SDS-PAGE) and probed with an anti-light chain antibody to assess the presence of anti-H3K27me3 antibody. After visualization, a single band with appreciable intensity was observed for each of the flow-through and bound fractions, suggesting both tested substrates captured the test antibody. Yet the polyacrylamide resin exhibited more complete, semi-quantitative binding of the test antibody, as compared to the magnetic beads (Figure 6C). Saturation of magnetic beads occurred between 2 and 5 μg of test antibody, as seen by corresponding bands of equal intensity in the bound fraction with the co-occurrence of a band in the flow-through fraction corresponding to 5 μg. Bands were absent in polyacrylamide resin flow-through for either amount of test antibody.

Having determined working parameters for ChIP, we assessed in high and low PPI groups levels of the activating H3ac mark at the proximal gene promoter of *Gapdh*. We found relative enrichment of H3ac levels over background at its gene promoter, with ChIP signal for H3ac levels, on average, accounting for ~7% of input in the low PPI group and ~6% in high PPI group, a difference found to be insignificant (Figure 7A). We also assessed levels of a repressive histone mark using a ChIP validated antibody specific for H3K27me3 in parallel with IgG as a negative

control. Between PPI groups, we detected low H3K27me3 levels at *Gapdh*, ~0.5% input for low PPI and ~0.4% input for high PPI (0.4% of input) groups, a statistically insignificant difference (Figure 7B). No qPCR signal was detected for IgG ChIP, validating the specificity of the binding to the H3K27me3 modification.

### CHROMATIN IP OF H3AC AND H3K27ME3 MARKS IN HIGH AND LOW PPI ANIMALS

We next set out to determine by ChIP if patterns of H3ac and H3K27me3 was associated with mRNA expression of *Grm2* in frontal cortex or *Drd2* in striatum which were indicated to contribute significantly to PPI response. Two-way ANOVA of H3ac or H3K27me3 ChIP at *Grm2* gene regions in frontal cortex did not show significant differences between low and high PPI animals (Figure 8). There was a main effect of gene region at *Grm2* on H3ac and H3K27me3 levels, though *post hoc* analysis did not reveal significant effects (for statistics, see Table 10). Two-way ANOVA of H3ac or H3K27me3 ChIP at *Drd2* gene regions in striatum did not show significant differences between low and high PPI animals (Figure 9). For H3ac, but not H3K27me3, there was a main effect of gene region, though *post hoc* analyses did not reveal significant effects on PPI response (Table 11).

To investigate a link between histone modifications and gene expression, we also assessed levels of H3ac and H3K27me3 at other genes that we found upregulated in frontal cortex of the low PPI group but did not correlate with PPI response *per se*. Two-way ANOVA of H3ac ChIP at *Drd2, Htr1a, Htr2a, and Homer1* gene regions did not show significant differences between low and high PPI animals (Figure 10), though an overall effect of gene region was noted for all tested targets. For H3K27me3 levels in the frontal cortex, a main effect of gene region was indicated for *Drd2* and *Homer1*, but not *Htr1a* or *Htr2a* (Figure 11). *Post hoc* analyses did not reveal a significant effect of H3ac or H3K27me3 modifications on PPI response (Table 10).

# CHAPTER 4: FIGURES

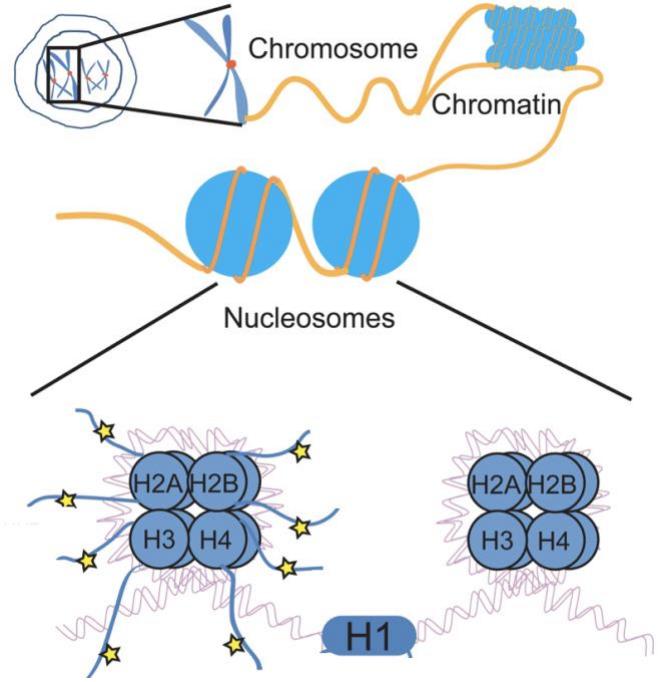


**FIGURE 1. CHROMATIN'S STRUCTURAL AND FUNCTIONAL UNIT IS THE NUCLEOSOME**

In eukaryotes, chromosomal DNA does not exist as a naked macromolecule. Instead it intertwines a core of highly basic histone proteins to form chromatin. This nucleoprotein complex collectively forms the structural and functional unit of chromatin called the nucleosome. Chromatin is then folded into higher-order structures, resulting in further genome compaction to fit inside the nucleus. The nucleosome consists of a histone core, an octameric assembly of two histone H2A/H2B dimers and a H3 and H4 tetramer. In addition, linker histone H1 binds regions of DNA on either side of a single nucleosome particle. Beyond a structural scaffold, more recently appreciated is that chromatin can regulate critical molecular functions via histone posttranslational modification of histones (*e.g.,* acetylation, methylation, phosphorylation, *etc.*). By installation of histone posttranslational modifications, it is thought that molecular processes including gene transcription can be epigenetically controlled. Source image reproduced with permission from (Wang et al., 2017).

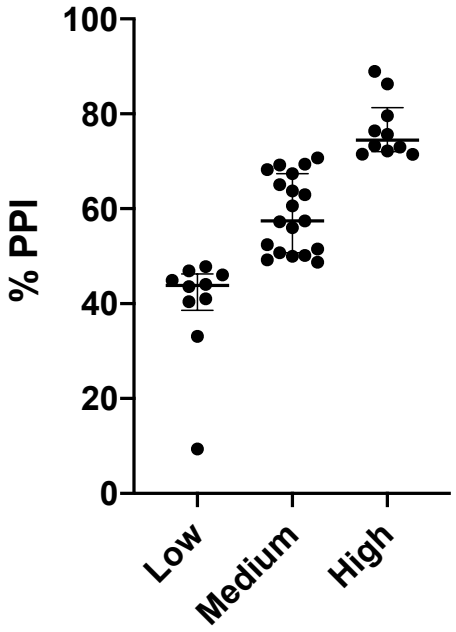


**FIGURE 2. SEGREGATION OF *NIH-HS* RATS INTO DIFFERENT PPI GROUPS**

*NIH-HS* rats were subsequently segregated into three groups based on PPI response (% PPI). Rats in the first and last quartile for PPI response (n=10 rats each) were segregated into low PPI and high PPI groups, respectively. Remaining animals (n=19) were placed in a medium PPI group. Collaborators at University of Copenhagen produced this figure. Reproduced with permission from (Østerbøg et al., 2019). For descriptive statistics of PPI groups, see Table 5 and Table 6.

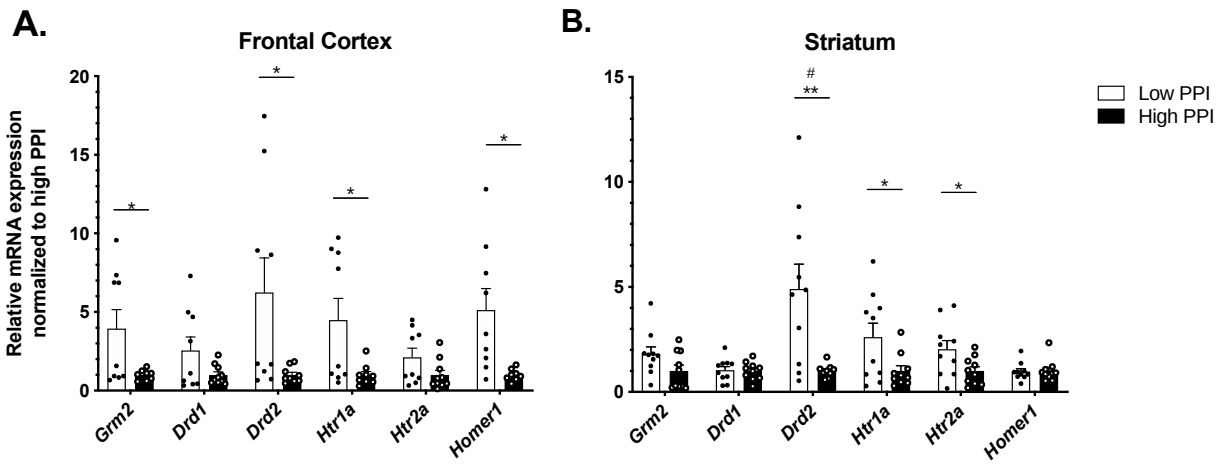


**FIGURE 3. MRNA EXPRESSION IN LOW AND HIGH PPI GROUPS**

**A.** mRNA expression of *Grm2*, *Drd2*, *Htr1a*, and *Homer1* was significantly increased in low PPI animals in frontal cortex. Differences did not pass multiple testing correction. **B.** mRNA expression of *Drd2*, *Htr1a*, and *Htr2a* was significantly increased in low PPI animals in the striatum, n=8 rats. Data are presented as mean ± s.e.m. Statistical significance was set at $p < 0.05$. *$p < 0.05$, **$p < 0.001$, $_{\#}p < 0.05$ after *post hoc* correction. Collaborators at University of Copenhagen produced this figure. Reproduced with permission from (Østerbøg et al., 2019). For t test statistics, see Table 8.

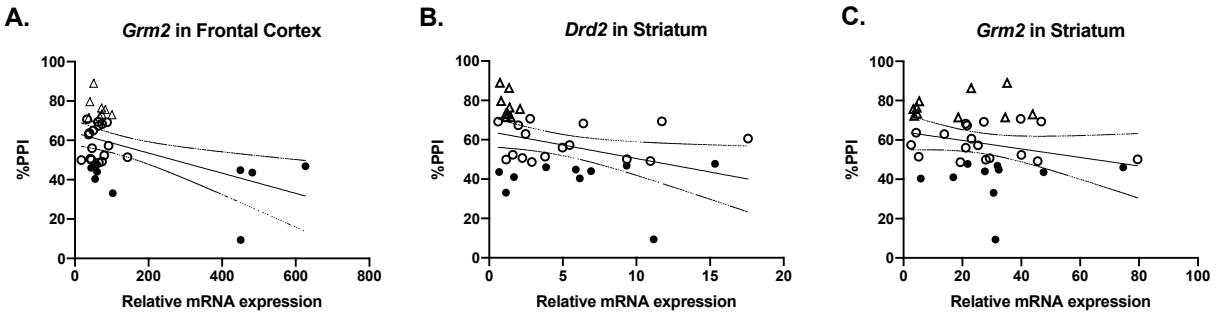


**FIGURE 4. REGRESSION ANALYSIS BETWEEN PPI RESPONSE AND MRNA EXPRESSION**

Linear regression analysis of PPI response (dependent variable) and mRNA expression (independent variable). **A.** *Grm2* expression levels in the frontal cortex correlate with PPI response ($R_2$ = 0.23; $p$ = 0.0043). **B.** *Drd2* expression levels in the striatum correlate with total PPI response ($R_2$ = 0.14; $p$ = 0.0286). Statistical significance was set at $p < 0.05$. Filled circles represent low PPI, open circles medium PPI and open triangles high PPI animals. For linear regression analysis statistics, see

Table 7. Collaborators at University of Copenhagen produced this figure. Reproduced with permission from (Østerbøg et al., 2019).

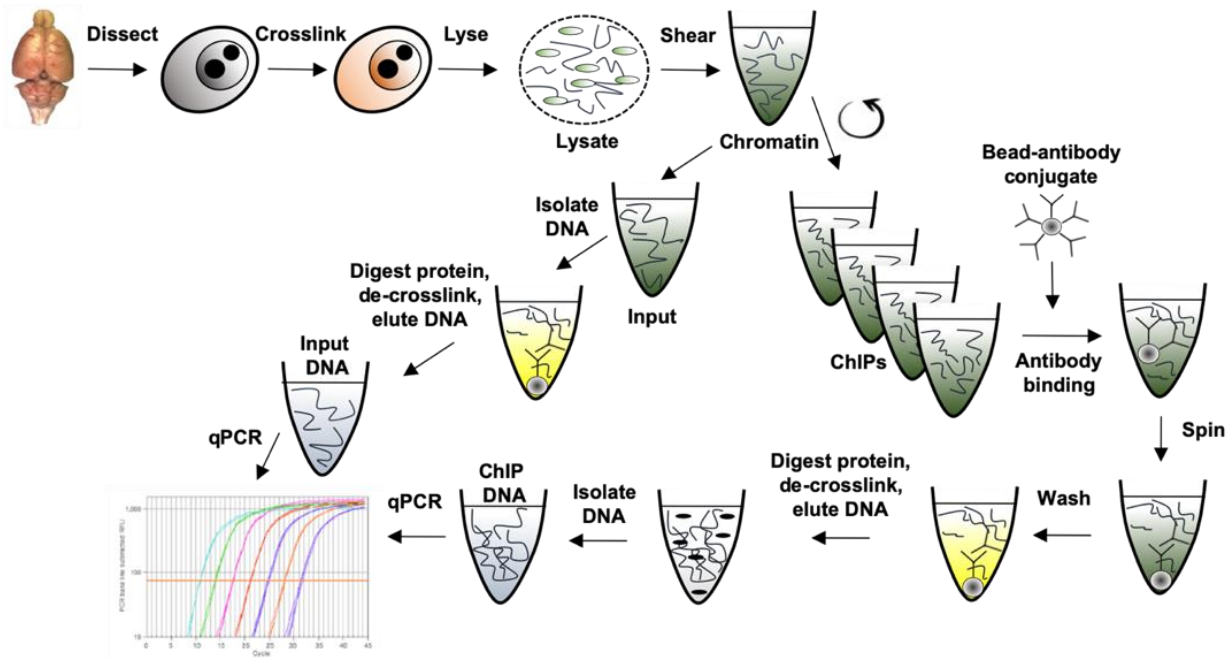


**FIGURE 5. CHROMATIN IMMUNOPRECIPITATION PROTOCOL**

Dissected tissue is treated with fixative to crosslink molecules *in situ*. Following lysis, crosslinked chromatin is released from nuclei and solubilized. Chromatin is subsequently sheared by sonication to produce fragments amenable to immunoprecipitation by antibodies selective for histone modifications. The chromatin-antibody complex—and the DNA associated to the histone modification—is retrieved by addition of beads and serially washed to eliminate non-specific interactions. Immunoprecipitated DNA is eluted, proteins are digested, and then crosslinks reversed. Purified DNA is isolated by phenol-chloroform extraction and ethanolic precipitation. Finally, abundance of immunoprecipitated DNA is quantified by qPCR assay and normalized to input DNA.

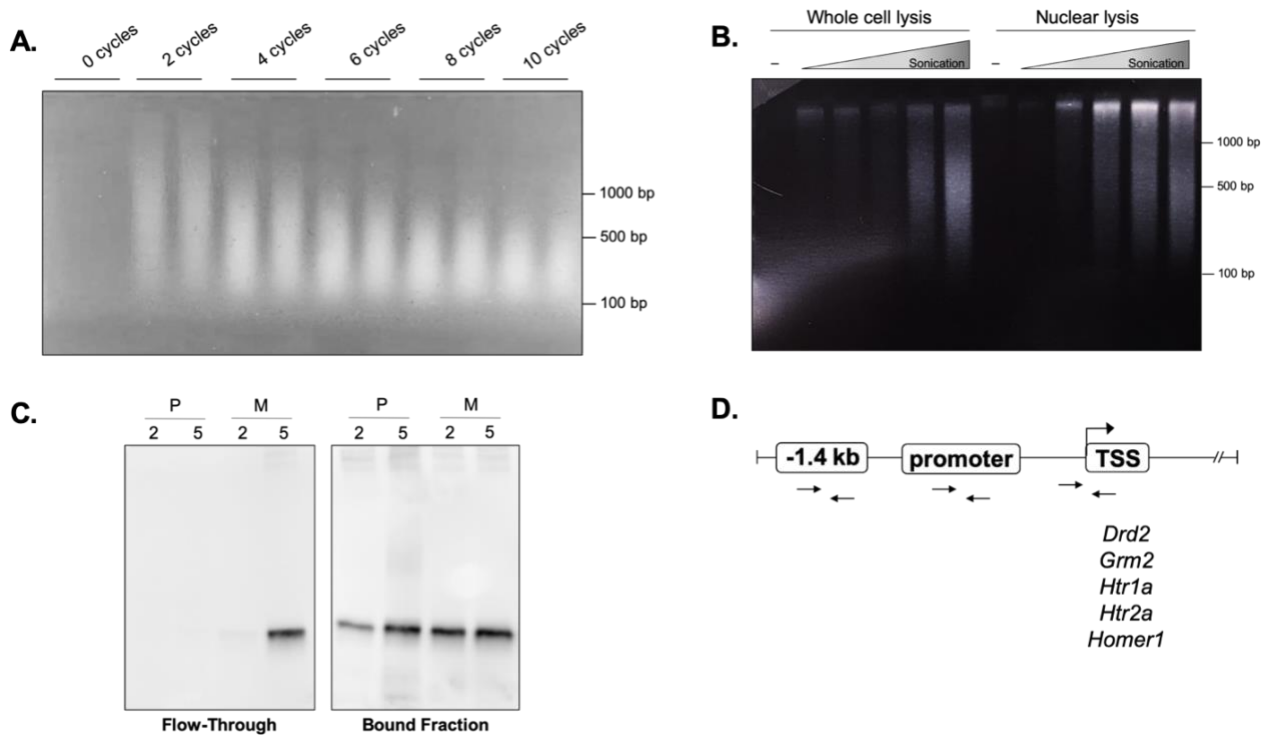


**FIGURE 6. PILOT STUDIES OF CHIP TECHNICAL PARAMETERS**

**A.** Representative DNA agarose gel showing effect of sonication cycle number on DNA fragment size. **B.** Representative DNA agarose gel showing resolution of sonicated DNA following whole cell lysis or hypotonic lysis. **C.** Western blot analysis with $\alpha$-$\kappa$ chain antibody comparing binding capacity of Protein A/G-linked polyacrylamide (P) and magnetic (M) substrates. Flow-through (left) shows unbound antibody. Bound fraction (right) shows antibody eluted from resin. Number above image indicates $\mu$g of ChIP antibody coupled to substrate. **D.** Schematic showing approximate genomic locations of ChIP-qPCR primer pairs for tested genes, as indicated below TSS, transcriptional start site.

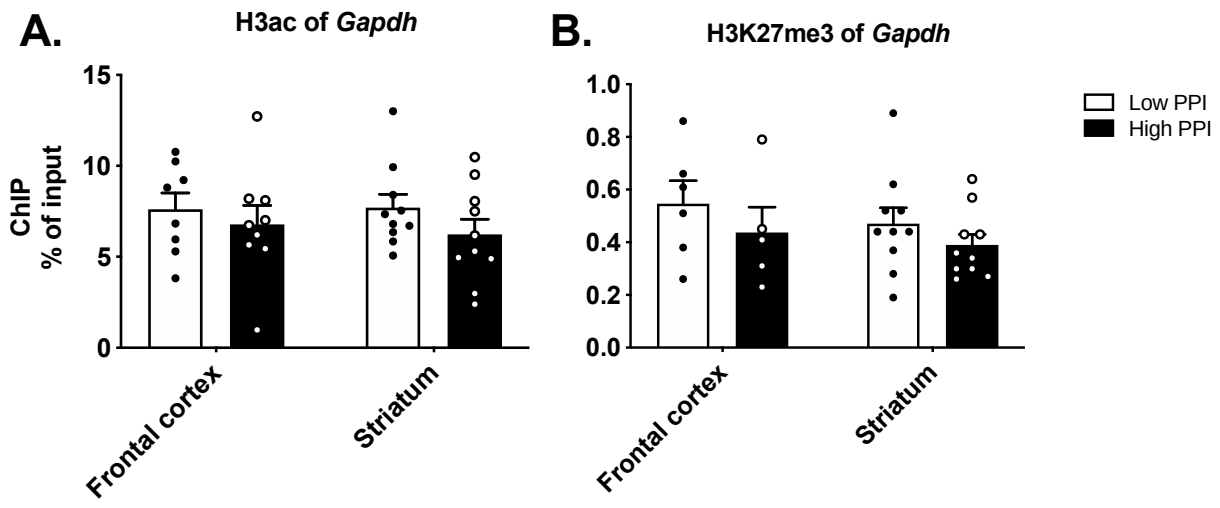


**FIGURE 7. H3AC AND H3K27ME3 LEVELS AT *GAPDH* PROMOTER**

In frontal cortex and striatum, levels of **(A)** H3ac and **(B)** H3K27me3 levels were not significantly different between low and high PPI groups. (A) H3ac, n=8-10 (B) H3K27me3 n=5-10. Statistical significance was set at $p < 0.05$. Data are presented as mean ± s.e.m. For Mann Whitney test statistics, see Table 9.

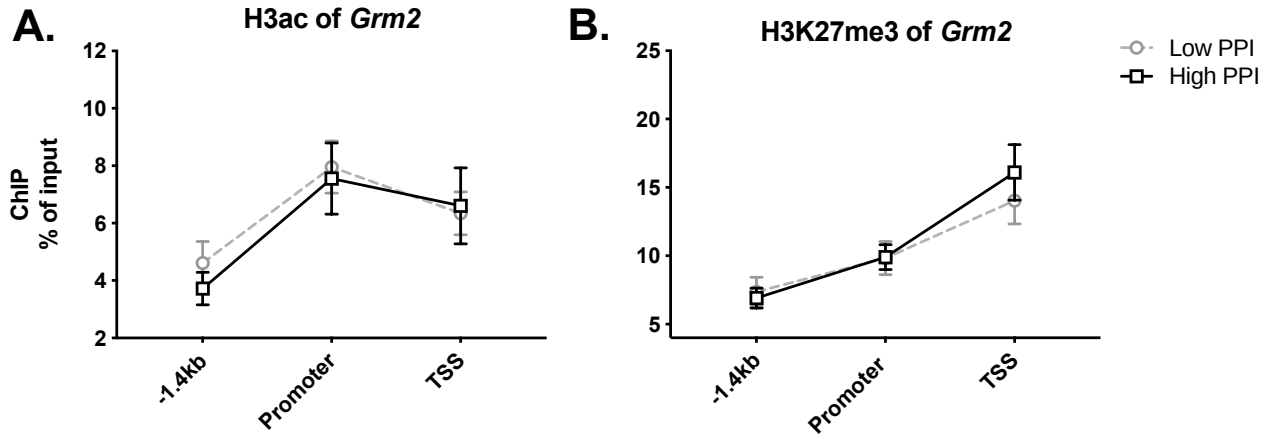


**FIGURE 8. H3AC AND H3K27ME3 LEVELS AT REGIONS OF *GRM2* IN FRONTAL CORTEX**

No significant difference in levels of **(A)** H3ac (n=5-6 rats) and **(B)** H3K27me3 (n=8-9 rats) at indicated *Grm2* gene regions in frontal cortex of low and high PPI animals. Statistical significance was set at $p < 0.05$. Data are presented as mean ± s.e.m. For two-way ANOVA with Holm-Šidák's multiple comparison test, see Table 10.

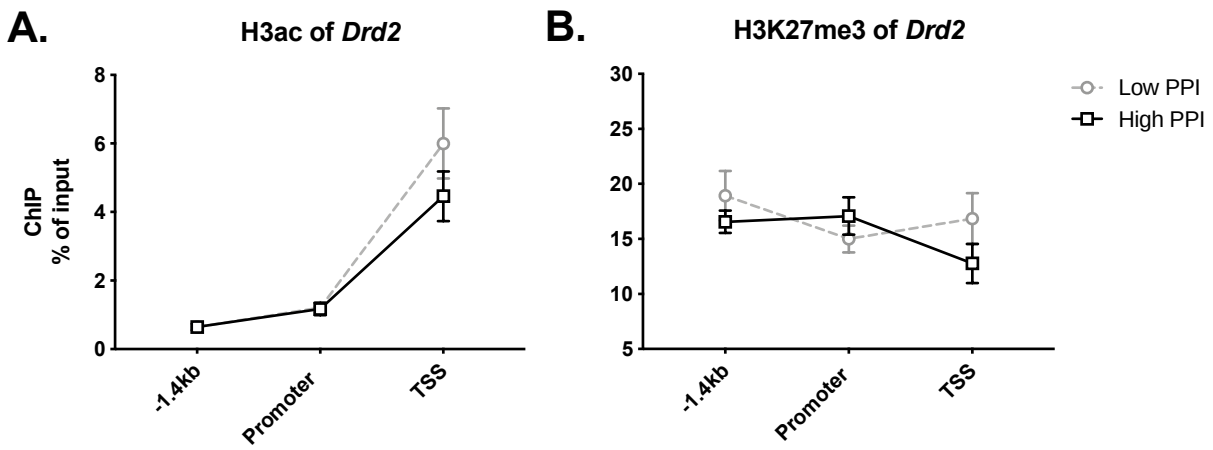


**FIGURE 9. H3AC AND H3K27ME3 LEVELS AT REGIONS OF *DRD2* IN STRIATUM**

No significant difference in levels of **(A)** H3ac (n=8 rats) and **(B)** H3K27me3 (n=5-6 rats) at indicated *Drd2* gene regions in striatum of low and high PPI animals. Statistical significance was set at $p < 0.05$. Data are presented as mean ± s.e.m. For two-way ANOVA with Holm-Šidák's multiple comparison test, see Table 11.

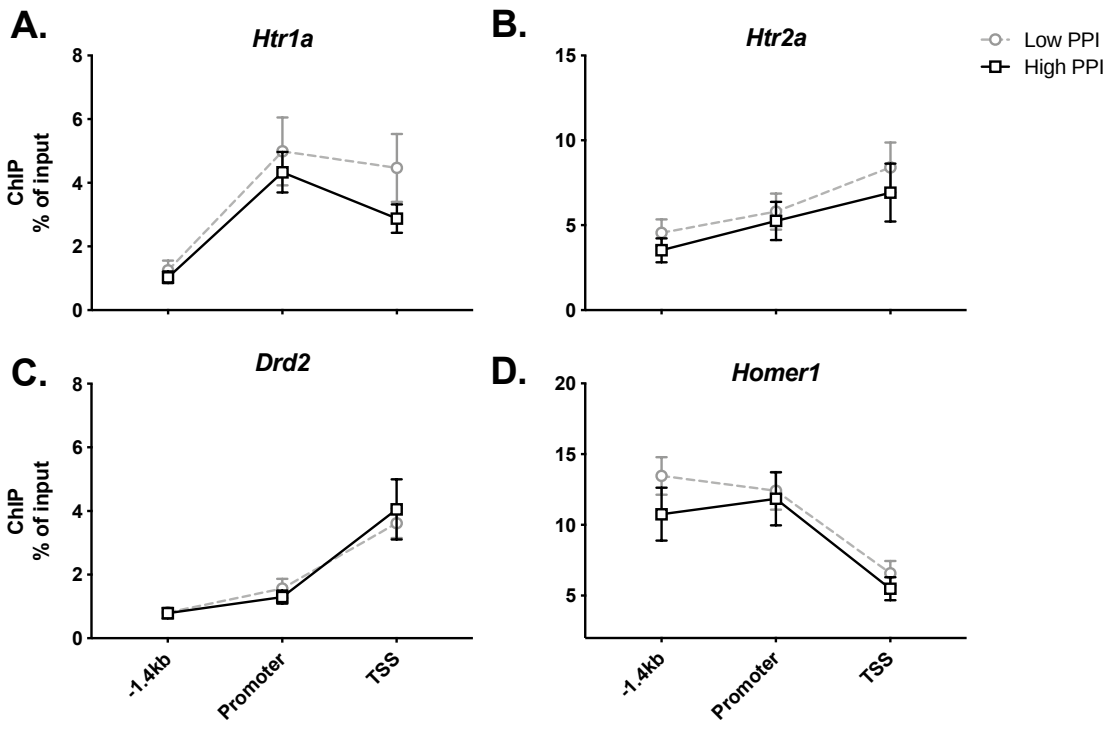


**FIGURE 10. H3AC LEVELS AT REGIONS OF GENES IN FRONTAL CORTEX**

No significant difference in levels of H3ac at upstream locations of indicated genes in frontal cortex of low and high PPI animals. Statistical significance was set at $p < 0.05$. *Htr1a*, n=8; *Htr2a*, n=5-6; *Homer1*, n=8 rats. Data are presented as mean ± s.e.m. For two-way ANOVA with Holm-Šidák's multiple comparison test, see Table 10.

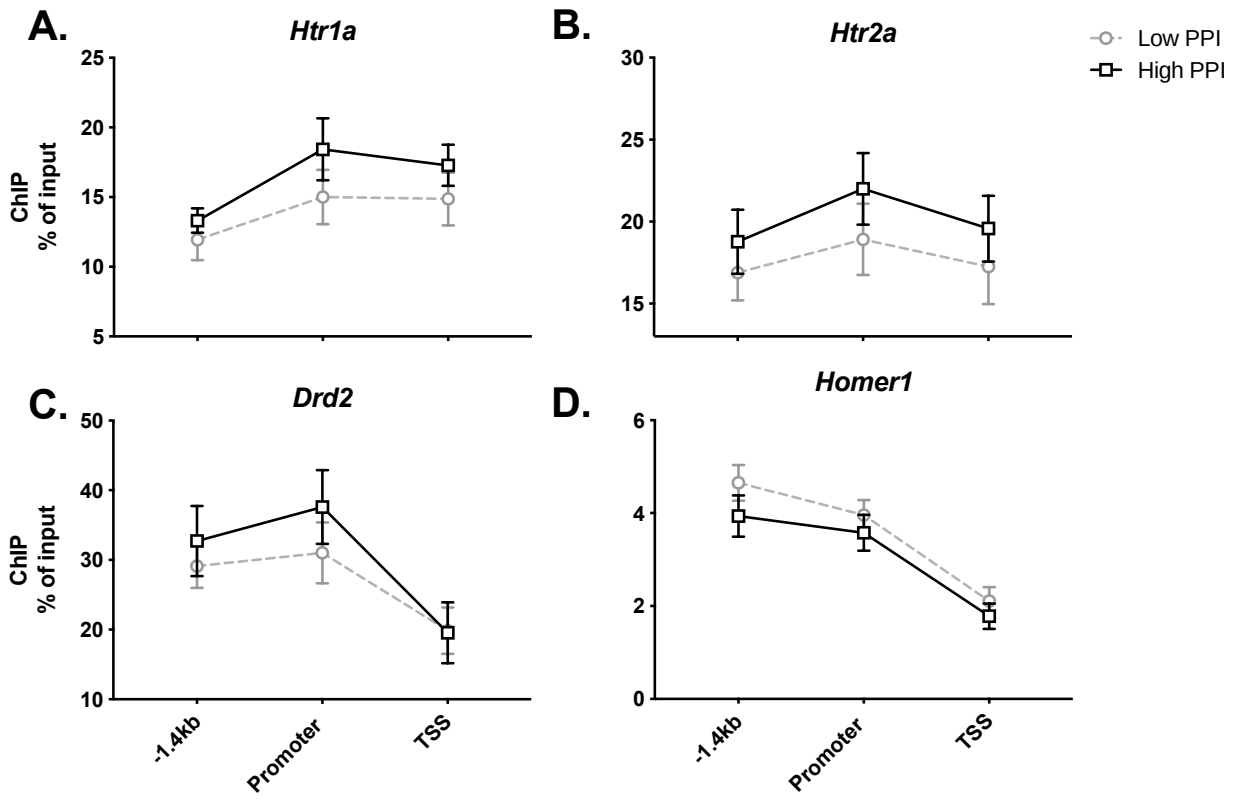


**FIGURE 11. H3K27ME3 LEVELS AT REGIONS OF GENES IN FRONTAL CORTEX**

No significant difference in levels of H3K27me3 at upstream locations of indicated genes in frontal cortex of low and high PPI animals. Statistical significance was set at $p < 0.05$. *Htr1a*, *Htr2a*, n=9; *Homer1*, n=5-6 rats. Data are presented as mean ± s.e.m. For two-way ANOVA with Holm-Šidák's multiple comparison test, see Table 10.

# CHAPTER 5. DISCUSSION

Here we report no difference in levels of H3ac or H3K27me3 between PPI groups across three upstream regions of *Grm2*, *Drd1*, *Drd2*, *Htr1a*, *Htr2a*, and *Homer1* of *HS* rats. The aim of the study was to assess in high and low PPI groups the relative abundance of two histone marks at DNA promoters of genes involved in sensorimotor gating regulation. We evaluated baseline levels of histone marks involved in gene transcription, namely activating H3ac and repressive H3K27me3. To this end, we adapted and validated a ChIP protocol for use in fixed frozen brain tissue.

### FEASIBILITY OF CHROMATIN IMMUNOPRECIPITATION IN FROZEN BRAIN TISSUE

Before setting out to test our hypothesis, we determined ideal parameters for the chromatin immunoprecipitation, or ChIP, protocol using frozen brain samples in a series of pilot studies. One of the most critical elements of a successful ChIP protocol—shearing of DNA—is also its most variable (Pchelintsev et al., 2016). To achieve this end, fixed samples can be subjected either to enzymatic digestion with micrococcal nuclease (MNase) (Telford and Stewart, 1989; Thorne et al., 2004) or to high-energy ultrasonic treatment. Both approaches have been used by our group successfully to shear DNA. Frozen tissues, such as post-mortem human brain, were unable to be sonically sheared and required MNase digestion to achieve appropriate DNA fragments (Kurita et al., 2012), and only freshly fixed, never frozen samples were amenable to the ChIP protocol. The use of ultrasonic treatment on frozen samples had yet to be addressed.

The general consensus in the literature suggests that chromatin be shared to fragments within the range of 200 to 1,000 bp (Rodríguez-Ubreva and Ballestar, 2014). Larger chromatin fragments may reduce the selectivity, as detected signals may be from more distant nucleosomes linked to target loci, while smaller fragments hinder the detection at all (Lee et al., 2006). Sonication for ChIP requires consideration of numerous factors, including cell or tissue type, degree of crosslinking, buffer composition, as well as parameters of the instrument used for sonication, including means of energy dispersal, power output, and process duration. To

determine that DNA shearing yielded chromatin fragments amenable to immunoprecipitation, we set out to determine appropriate number of sonication cycles, including power output and time intervals between active ultrasound treatment. It is also noteworthy that as all polymeric macromolecules are subject to ultrasound-mediated shearing, samples at this stage comprise a crude mixture of fragments, requiring further processing (*e.g.*, removal of insoluble debris, RNase and proteinase treatment, and crosslink reversal). Limited by starting tissue quantity, we opted to minimize loss by precipitating DNA following organic extraction instead of using spin-columns where an appreciable amount of sample can be lost on the silica matrix.

We also focused on determining conditions that would solubilize sufficient chromatin from crosslinked tissues for subsequent fragmentation. Isolation of nuclei from tissues yielded a sufficient fraction of soluble chromatin post-sonication. Interestingly, we noted a relatively intense population of slow-migrating DNA species under nuclear lysis that was less apparent under whole cell lysis. The apparently higher amount of soluble DNA under the whole cell lysis conditions may be due to the presence of SDS, which is otherwise absent in the nuclear lysis buffer.

We also determined that use of polyacrylamide resin was ideal for our samples. Based on our findings and in consideration of the limited amount of soluble chromatin available from nuclear lysis, we proceeded to use polyacrylamide resin with the higher amount of ChIP-grade antibody. These findings may be because polyacrylamide resin is porous and has a large surface-area-to-volume ratio and therefore a high binding capacity. On the other hand, magnetic beads are nonporous, and, although they are smaller in diameter, may exhibit a lower binding capacity than polyacrylamide resin.

To validate our ChIP protocol, we assessed abundance of H3ac and H3K27me3 levels at *Gapdh*. We observed relative enrichment of activating H3ac and scant levels of repressive H3K27me3 marks, relative to IgG background at the proximal promoter region of *Gapdh*. As a housekeeping gene, *Gapdh* is constitutively expressed and its gene promoter is expected to bear marks associated with active gene transcription, including lysine acetylation of H3. There remains

the possibility that patterns of H3ac and H3K27me3 found at *Gapdh* across two brain regions were spurious. The presence of pan-acetylated H3 or absence of H3K27me3 at one gene locus may be insufficient evidence our ChIP protocol is operational, though another study has previously reported similar patterns of histone PTMs at *Gapdh* (Fomsgaard et al., 2018). Further investigations into abundance of additional histone modifications, including specific acetylated lysine residues, like H3K9ac and or H3K27ac, as well as other repressive marks, like H3K9me3 or H4K20me3, at other transcriptionally active loci, including *Gapdh,* are warranted. Unbiased approaches like deep sequencing of the epigenome may yet offer clarify in this case and at large.

### EPIGENETIC ALTERATIONS IN SYNAPTIC PLASTICITY GENES

The ability to 'gate' irrelevant stimuli while also attending to those relevant is an important and subconscious process of the central nervous system. Impairments in sensorimotor gating are considered a clinical endophenotype shared across several diagnostic domains of neuropsychiatric conditions (Owens et al., 2011). Deficits in this protective cognitive process are operationally defined by deficits in the prepulse inhibition of acoustic startle. Various approaches, including behavioral animal models, pharmacological dissection, and gene linkage and genome wide association studies have identified key neurobiological substrates regulating PPI, for instance, revealing a role for monoamine neurotransmitter receptors, as well as synaptic and neural plasticity genes in neurocircuits encompassing forebrain and midbrain structures. Despite steady contributions made over decades to understand the neurobiology of prepulse inhibition, viable therapeutic strategies from the bench did not translate to the clinic. With its polygenic inheritance pattern, variable phenotypic expressivity, and distributed neuroanatomical circuit, efforts to dissect the molecular mechanism of sensorimotor gating have remained elusive to date.

Ample evidence has shown monoamine neurotransmitter systems are involved in the regulation of sensorimotor gating. The gene products of *Drd1*, *Drd2*, *Htr1a*, *Htr2a*, and *Grm2* are psychotropic drug targets. It is also noteworthy that the neurobiology of the PPI response has been dissected with pharmacological agents targeting neurotransmitter systems studied here, as

with *Grm2* (Bellesi and Conti, 2010; van Berckel et al., 2006) and *Htr1a* (Conti, 2012). Given that receptor mRNA is separable from consequent behavior-associated functions, it is possible that events beyond post-transcriptional regulation by histone PTMs plays a more direct mediating role in PPI response which is subject to processes of synaptic plasticity. For instance, the *Homer1* gene product regulates the functional assembly of post-synaptic density proteins at glutamatergic synapses to influence synaptic plasticity. Animals that lack *Homer1* exhibit schizophrenia-like behaviors, including diminished PPI response (Datko et al., 2017). As a behavioral phenotype with translational value, if the PPI paradigm is in part epigenetically regulated, understanding the relationship between gene expression and histone modification can provide insight into the pathophysiology of other CNS disorders with deficits in inhibitory control processes.

In *RHA* rats, a putative model of PPI deficiency, higher H3K27me3 levels at the *Htr2a* gene promoter in the striatum was correlated with decreased *Htr2a* mRNA (Fomsgaard et al., 2018). This raised the possibility that baseline differences in histone modification are associated with altered gene expression relevant to PPI response. The present study in genetically distinct animals however was underpowered for robust regression analysis. Future studies using genetically diverse models are warranted to address a role for interindividual differences mediating the PPI response.

Rationalized therapeutic insights into a complex, polygenic trait like PPI deficiency using highly inbred animal models may be circumscribed by a diminished pool of allelic variation stemming from many generations of inbreeding, drift, and fixation. Like other complex psychiatric conditions (Pierce et al., 2018; Ponomarev et al., 2012), PPI response is likely regulated by a number of genes and gene networks, including those tested here. To address this limitation, we used rats from a genetically heterogeneous stock. The *HS* model has been used to fine-map complex traits of numerous conditions, ranging from diabetes and heart disease to anxiety and drug abuse behaviors (Baud et al., 2013). This outbred stock features animals that bear a high degree of genetic mosaicism and manifest the breadth of phenotypic traits, notably including PPI

response explored here. More studies conducted will be needed to determine modifiable trait loci in phenotypically diverse populations and the epigenetic modifications regulating them. Moreover, genetic findings offer clues as to which molecular networks undergird associations to the impaired PPI response, thus expanding the molecular drug target space for exploration in drug discovery. Coupled with a reverse genetic approach, like Crispr-Cas9-mediated gene-editing, *HS* animals can be a yet more powerful model to further pinpoint the genetic and epigenetic correlates of complex behaviors in rats that may have translational relevance to neuropsychiatric conditions in humans.

These findings also do not exclude the involvement of other genes in histone PTMs in transcriptional regulation of tested genes. We focused on frontal cortex and striatum, two forebrain structures that have been shown to regulate the PPI response. These findings suggest that neither histone modification within the frontal cortex and striatum contributes to the difference in PPI response. Studies looking at other regions like the hippocampus may be worthwhile. Furthermore, additional studies looking at other gene targets are warranted. Clinical studies of PPI dysfunction have implicated certain gene variants that can impact the course and severity of dysfunction via influences on neurotransmitter systems, neurocircuitry, cellular physiology, neurodevelopment, and other traits that culminate in appropriate behaviors. Other mechanisms, such as epigenetic regulation by DNA methylation or microRNAs, may be operable. We present these negative findings to underscore the importance of further investigations into epigenetic mechanisms that may offer insight into potential molecular pathways contributing to baseline patterns of gene expression of complex behaviors, including PPI.

The notion that the epigenome is druggable is feasible and has been explored. For over thirty years now, azacytidine has been used in the treatment of hematologic malignancies. It was thought that as an inhibitor of DNA methyltransferase, azacytidine exerted its anti-tumor effect by thwarting the epigenetic process of post-replicative DNA methylation, thereby triggering DNA damage pathways. More recent studies have revealed a parallel mechanism of action, whereby

an intrinsic toxic antiviral response is elicited via transcriptional activation of endogenous retroviral sequences (Licht, 2015). Another case of an epigenetic target was also originally developed against hematologic malignancies and targets histone deacetylase complexes. These and other enzymes that reversibly modify the chromatin landscape are enticing drug targets. Inhibitors of HDACs have shown therapeutic promise in neurological and neurodegenerative disorders, like Alzheimer's, Huntington's, and Parkinson's disease (Dietz and Casaccia, 2010; Penney and Tsai, 2014), although not without risks of side effects. Given the intricate and interconnected molecular architecture of neuropsychiatric conditions (Gandal et al., 2018; Gratten et al., 2014), an unknown number of genes are likely contributing to the PPI response. Epigenomic profiling by ChIP sequencing may reveal distinct disease signatures to narrow the search window of the disease-relevant genetic substrates. At present, however, targeted manipulation of particular histone PTMs as a therapeutic modality remains an aspirational and distant prospect. Concerted efforts will be needed to more fully characterize how chromatin-templated processes acting 'above the genes' interact with the genes themselves, ultimately to manifest as a phenotype with consequential health effects. Novel therapeutic rationales for wide-ranging disorders including neuropsychiatric conditions may lie in wait amidst the dynamic and complex landscape of the epigenome.

# APPENDIX

**TABLE 2. RT-QPCR OLIGONUCLEOTIDE SEQUENCES (*RATTUS NORVEGICUS*)**

| Gene (Accession ID) | DNA Sequence (5' to 3') |
|---|---|
| *Gapdh* (NM_017008.4) | F: CATCAAGAAGGTGGTGAAGCA |
| | R: CTGTTGAAGTCACAGGAGACA |
| *Rpl13a* (NM_173340.2) | F: AGCAGCTCTTGAGGCTAAGG |
| | R: GGGTTCACACCAAGAGTCCA |
| *Grm2* (NM_001105711.1) | F: GTGGTGACATTGCGCTGTAA |
| | R: GCGATGAGGAGCACATTGTA |
| *Drd1* (NM_012546.2) | F: GGAGGACACCGAGGATGA |
| | R: ATGAGGGACGATGAAATGG |
| *Drd2* (NM_012547.1) | F: TCGAGCTTTCAGAGCCAACC |
| | R: GGGTACAGTTGCCCTTGAGTG |
| *Htr1a* (NM_012585.1) | F: CCAAGAAGAGCCTGAACGGA |
| | R: CTGCCTCACTGCCCCATTAG |
| *Htr2a* (NM_017254.1) | F: CCGCTTCAACTCCAGAACCA |
| | R: GATTGGCATGGATATACCTACAGA |
| *Homer1* (AJ276327.1) | F: CACCCGATGTGACACAGAACTC |
| | R: TGATTGCTGAATTGAATGTGTACCT |

**TABLE 3. RECOMMENDED THERMOCYCLE PROFILES FOR RT-QPCR**

**Standard Cycling Mode (Primer $T_m$ ≥60°C)**

| Step | Temp | Duration | Cycles |
|---|---|---|---|
| UDG Activation | 50˚C | 2 min | Hold |
| AmpliTag® DNA Polymerase | 95˚C | 2 min | Hold |
| Denature | 95˚C | 15 sec | 40 |
| Anneal/Extend | 60˚C | 1 min | |

**Standard Cycling Mode (Primer $T_m$ < 60°C)**

| Step | Temp | Duration | Cycles |
|---|---|---|---|
| UDG Activation | 50˚C | 2 min | Hold |
| AmpliTag® DNA Polymerase | 95˚C | 2 min | Hold |
| Denature | 95˚C | 15 sec | 40 |

| | | |
|---|---|---|
| Anneal | 55-60˚C | 15 sec |
| Extend | 72˚C | 1 min |

Reproduced from page 18 of https://assets.thermofisher.com/TFS-Assets/LSG/manuals/4472919_4473367_SYBR_Select_MasterMix_UG.pdf

**TABLE 4. CHIP-QPCR OLIGONUCLEOTIDE SEQUENCES (*RATTUS NORVEGICUS*)**

| Gene (Accession ID) | DNA Sequence (5' to 3') | Location |
|---|---|---|
| *Grm2* (NC_005107.4) | F: GGCAGAGCTGGATCTGGAAG<br>R: AATGGGAGACAAGGTGGCAG | Distal promoter |
| | F: ATTCAGCACCACAAGGTGGACA<br>R: CAATTTGGCCTGCACCTCTCGC | Proximal promoter |
| | F: ATGAGCACCGAGGCATACAG<br>R: GATGCGGTCCAGTGCAAAAA | TSS |
| *Htr1a* (NC_005101.4) | F: CGGGTGCTGAACCAAATTTCA<br>R: TTGGTGGCATCCCTTGTCTT | Distal promoter |
| | F: CTTCGCCCGAGCAAGTAAGA<br>R: TTCAGAGGGAGGGGATCCAG | Proximal promoter |
| | F: TCCACTTTCGGCGCTTTCTA<br>R: TGACAGTCTTGCGGATTCGG | TSS |
| *Htr2a* (NC_005114.4) | F: ACTGGTGTGGGCTAGAAGTGC<br>R: GAGGGGCGAAGTGTGAGAAAA | Distal promoter |
| | F: ACACGTTTGTGTCCCCGAAT<br>R: AACATGTGTGGCTCCTCTGG | Proximal promoter |
| | F: TTCGGAAGCATCGAACTGGA<br>R: AGAATGGAGAGGGCATGTCGG | TSS |
| *Drd2* (NC_005107.4) | F: ACATCTACAACTGGCAAGGGA<br>R: GTTTTCCACCCAGTCGTGTG | Distal promoter |
| | F: AGTGCTTCAGCTAGCCCTTG<br>R: GGGGAAGGAACCTTGAGAGC | Proximal promoter |
| | F: TGTACAAGGGGCGGGGTT<br>R: CACAAGAGGGGACCAGCC | TSS |
| *Homer1* (NC_005101.4) | F: GAGTAACCTGGCTGCTTGAGT<br>R: GTTGCGCGGAGAATATAGCAC | Distal promoter |
| | F: TTAGCCCAAAGGCCGAGTAA<br>R: GCTGATCATTTCGCTCACGTC | Proximal promoter |
| | F: AGCGAGAGAAACCAGAGCAG<br>R: CGGCCGGAAGTACTGCTAAA | TSS |
| *Gapdh* (NC_005103.4) | F: AACCCTCATCCGGTCACTTCC<br>R: CGAGTAGCTGGGCCTCTCTCA | Proximal promoter |

**TABLE 5. COLUMN STATISTICS OF PPI RESPONSE OF PPI GROUPS**

| PPI Group | n | Minimum | 1st Quartile | Median | 3rd Quartile | Maximum |
|---|---|---|---|---|---|---|
| Low | 10 | 9.39 | 38.58 | 43.85 | 46.27 | 47.8 |
| Medium | 19 | 48.71 | 50.7 | 57.43 | 67.38 | 70.71 |
| High | 10 | 71.46 | 72.02 | 74.46 | 81.27 | 88.92 |

**TABLE 6. PPI RESPONSE OF PPI GROUPS TO DIFFERENT PREPULSE INTENSITIES**

| Stimulus | Low PPI | Medium PPI | High PPI | Kruskal-Wallis H | *p* value |
|---|---|---|---|---|---|
| Baseline* | 369.0 ± 75.33# | 775.80 ± 217.80 | 981.90 ± 193.10 | 6.981 | 0.0305 |
| $\%PPI_{65\ dB}$**** | 8.66 ± 10.57#### | 42.55 ± 2.81 | 70.94 ± 3.01 | 28.36 | < 0.0001 |
| $\%PPI_{70\ dB}$**** | 41.48 ± 4.38#### | 53.63 ± 2.90 | 76.07 ± 2.52 | 22.20 | < 0.0001 |
| $\%PPI_{75\ dB}$**** | 51.07 ± 3.30#### | 66.55 ± 2.13 | 77.36 ± 2.73 | 18.82 | < 0.0001 |
| $\%PPI_{80\ dB}$*** | 57.71 ± 4.77### | 73.20 ± 3.15 | 82.91 ± 1.52 | 16.69 | < 0.0001 |
| $\%PPI_{total}$**** | 39.73 ± 3.63#### | 59.98 ± 1.82 | 76.82 ± 1.98 | 32.35 | < 0.0001 |

Kruskal-Wallis test with *post hoc* Dunn's multiple comparison test. $\%PPI_{total}$ represents mean % PPI score for different prepulse intensities. (*)Asterisk denotes significant difference in PPI response across the three groups. # denotes significant difference between low and high of PPI groups following *post hoc* analysis. Low PPI, n=10; medium PPI, n=19; high PPI, n=10 rats. Data is presented as mean ± s.e.m. Statistical significance was set at $p < 0.05$. *$p \leq 0.05$ ***$p \leq 0.001$, ****$p < 0.0001$, #$p \leq 0.05$, ###$p \leq 0.001$, ####$p < 0.0001$ (after Dunn's *post hoc* correction)

**TABLE 7. MULTINOMIAL LOGISTIC REGRESSION ANALYSIS OF PPI RESPONSE & MRNA LEVELS**

| Brain Region | Gene | -2 log likelihood of reduced model | *Likelihood ratio tests* | | |
|---|---|---|---|---|---|
| | | | **χ2** | **df** | ***p* value** |
| Frontal cortex | *Grm2* | 48.047 | 8.239 | 2 | 0.016 |
| | *Htr1a* | 42.722 | 2.915 | 2 | 0.233 |
| | *Htr2a* | 40.288 | 0.481 | 2 | 0.786 |
| | *Drd1* | 44.292 | 4.485 | 2 | 0.106 |
| | *Drd2* | 43.291 | 3.483 | 2 | 0.175 |
| | *Homer1* | 42.288 | 2.480 | 2 | 0.289 |
| Striatum | *Grm2* | 49.154 | 7.722 | 2 | 0.021 |
| | *Htr1a* | 46.294 | 4.862 | 2 | 0.088 |
| | *Htr2a* | 41.917 | 0.486 | 2 | 0.784 |

| | | | | |
|---|---|---|---|---|
| *Drd1* | 45.545 | 4.113 | 2 | 0.128 |
| *Drd2* | 57.260 | 15.829 | 2 | 0.000 |
| *Homer1* | 45.519 | 4.087 | 2 | 0.130 |

**TABLE 8. MULTIPLE T TESTS WITH HOLM-ŠIDÁK'S MULTIPLE CORRECTIONS: GENE EXPRESSION**

| Brain Region | Gene | *p* value | Adj. *p* value |
|---|---|---|---|
| Frontal cortex | *Grm2* | 0.0771 | 0.2140 |
| | *Drd1* | 0.8659 | 0.9820 |
| | *Drd2* | 0.0062 | 0.0365 |
| | *Htr1a* | 0.0340 | 0.1590 |
| | *Htr2a* | 0.0360 | 0.1590 |
| | *Homer1* | 0.8965 | 0.9820 |
| Striatum | *Grm2* | 0.0368 | 0.1173 |
| | *Drd1* | 0.0802 | 0.1540 |
| | *Drd2* | 0.0299 | 0.1173 |
| | *Htr1a* | 0.0246 | 0.1173 |
| | *Htr2a* | 0.0882 | 0.1540 |
| | *Homer1* | 0.0122 | 0.0711 |

**TABLE 9. MANN-WHITNEY TESTS OF H3AC AND H3K27ME3 CHIP (*GAPDH* PROMOTER)**

| Brain Region | Histone Mark | Mann-Whitney U | *p* value |
|---|---|---|---|
| Frontal cortex | H3ac | 33 | 0.2176 |
| | H3K27me3 | 33 | 0.2103 |
| Striatum | H3ac | 30 | 0.6058 |
| | H3K27me3 | 10 | 0.4286 |

**TABLE 10. TWO-WAY ANOVA OF H3AC AND H3K27ME3 CHIP IN FRONTAL CORTEX**

| Histone Mark | Gene | Variation | F(dfn, dfd) | *p* value | *Holm-Šídák post hoc* Gene Region | *Holm-Šídák post hoc* Adj *p* value |
|---|---|---|---|---|---|---|
| H3ac | *Grm2* | Interaction | F(2,46) = 0.171 | 0.8435 | -1.4kb | 0.9029 |
| | | Gene region | F(2,46) = 6.600 | 0.0030 | Promoter | 0.9881 |
| | | PPI | F(1,46) = 0.182 | 0.6716 | TSS | 0.9965 |
| | *Drd2* | Interaction | F(2,42) = 0.2950 | 0.7461 | -1.4kb | > 0.9999 |
| | | Gene region | F(2,42) = 23.81 | < 0.0001 | Promoter | 0.9684 |
| | | PPI | F(1,42) = 0.0166 | 0.8981 | TSS | 0.8837 |
| | *Htr1a* | Interaction | F(2,42) = 0.491 | 0.6153 | -1.4kb | 0.9948 |

| | | | | | | |
|---|---|---|---|---|---|---|
| | | Gene region | F(2,42) = 13.20 | < 0.0001 | Promoter | 0.8853 |
| | | PPI | F(1,42) = 2.035 | 0.1611 | TSS | 0.3157 |
| | | Interaction | F(2,28) = 0.080 | 0.9237 | -1.4kb | 0.8861 |
| | *Htr2a* | Gene region | F(2,28) = 4.841 | 0.0156 | Promoter | 0.9799 |
| | | PPI | F(1,28) = 1.190 | 0.2846 | TSS | 0.7813 |
| | | Interaction | F(2,42) = 0.311 | 0.7341 | -1.4kb | 0.4550 |
| | *Homer1* | Gene region | F(2,42) = 12.35 | < 0.0001 | Promoter | 0.9893 |
| | | PPI | F(1,42) = 1.589 | 0.2145 | TSS | 0.9293 |
| | | Interaction | F(2,27) = 0.474 | 0.6275 | -1.4kb | 0.9937 |
| | *Grm2* | Gene region | F(2,27) = 17.43 | < 0.0001 | Promoter | > 0.9999 |
| | | PPI | F(1,27) = 0.250 | 0.6208 | TSS | 0.6491 |
| | | Interaction | F(2,27) = 0.332 | 0.7204 | -1.4kb | 0.9114 |
| | *Drd2* | Gene region | F(2,27) = 6.495 | 0.0050 | Promoter | 0.6290 |
| | | PPI | F(1,27) = 0.905 | 0.3499 | TSS | > 0.9999 |
| | | Interaction | F(2,24) = 0.180 | 0.8361 | -1.4kb | 0.9239 |
| H3K27me3 | *Htr1a* | Gene region | F(2,24) = 3.330 | 0.0529 | Promoter | 0.4275 |
| | | PPI | F(1,24) = 2.967 | 0.0978 | TSS | 0.6948 |
| | | Interaction | F(2,24) = 0.043 | 0.9581 | -1.4kb | 0.8903 |
| | *Htr2a* | Gene region | F(2,24) = 0.904 | 0.4184 | Promoter | 0.6567 |
| | | PPI | F(1,24) = 2.098 | 0.1604 | TSS | 0.8173 |
| | | Interaction | F(2,27) = 0.174 | 0.8414 | -1.4kb | 0.4242 |
| | *Homer1* | Gene region | F(2,27) = 23.83 | < 0.0001 | Promoter | 0.8426 |
| | | PPI | F(1,27) = 2.643 | 0.1156 | TSS | 0.8903 |

**TABLE 11. TWO-WAY ANOVA OF H3AC AND H3K27ME3 CHIP IN STRIATUM (*DRD2*)**

| | | | | *Holm-Šídak post hoc* | |
|---|---|---|---|---|---|
| **Histone Mark** | **Variation** | **F(dfn, dfd)** | ***p* value** | **Gene Region** | **Adj *p* value** |
| | Interaction | F(2,51) = 0.1901 | 0.827 | -1.4kb | 0.929 |
| H3ac | Gene region | F(2,51) = 85.55 | < 0.0001 | Promoter | 0.9529 |
| | PPI | F(1,51) = 1.751 | 0.192 | TSS | 0.4911 |
| | Interaction | F(2,53) = 1.540 | 0.224 | -1.4kb | 0.7248 |
| H3K27me3 | Gene region | F(2,53) = 1.372 | 0.262 | Promoter | 0.8097 |
| | PPI | F(1,53) = 0.985 | 0.326 | TSS | 0.2992 |

# REFERENCES


Ahmari, S.E., Risbrough, V.B., Geyer, M.A., and Simpson, H.B. (2012). Impaired Sensorimotor Gating in Unmedicated Adults with Obsessive–Compulsive Disorder. Neuropsychopharmacology *37*, 1216–1223.

Andrews, A.J., and Luger, K. (2011). Nucleosome Structure(s) and Stability: Variations on a Theme. Annu. Rev. Biophys. *40*, 99–117.

Baldan Ramsey, L.C., Xu, M., Wood, N., and Pittenger, C. (2011). Lesions of the dorsomedial striatum disrupt prepulse inhibition. Neuroscience *180*, 222–228.

Bannister, A.J., and Kouzarides, T. (2011). Regulation of chromatin by histone modifications. Cell Res. *21*, 381–395.

Barski, A., Cuddapah, S., Cui, K., Roh, T.-Y., Schones, D.E., Wang, Z., Wei, G., Chepelev, I., and Zhao, K. (2007). High-resolution profiling of histone methylations in the human genome. Cell *129*, 823–837.

Baud, A., Hermsen, R., Guryev, V., Stridh, P., Graham, D., McBride, M.W., Foroud, T., Calderari, S., Diez, M., Ockinger, J., et al. (2013). Combined sequence-based and genetic mapping analysis of complex traits in outbred rats. Nat. Genet. *45*, 767–775.

Baylin, S.B., and Jones, P.A. (2011). A decade of exploring the cancer epigenome - biological and translational implications. Nat. Rev. Cancer *11*, 726–734.

Bellesi, M., and Conti, F. (2010). The mGluR2/3 Agonist LY379268 Blocks the Effects of GLT-1 Upregulation on Prepulse Inhibition of the Startle Reflex in Adult Rats. Neuropsychopharmacology *35*, 1253–1260.

van Berckel, B.N.M., Kegeles, L.S., Waterhouse, R., Guo, N., Hwang, D.-R., Huang, Y., Narendran, R., Van Heertum, R., and Laruelle, M. (2006). Modulation of amphetamine-induced dopamine release by group II metabotropic glutamate receptor agonist LY354740 in non-human primates studied with positron emission tomography. Neuropsychopharmacol. Off. Publ. Am. Coll. Neuropsychopharmacol. *31*, 967–977.

Borrelli, E., Nestler, E.J., Allis, C.D., and Sassone-Corsi, P. (2008). Decoding the Epigenetic Language of Neuronal Plasticity. Neuron *60*, 961–974.

Braff, D., Stone, C., Callaway, E., Geyer, M., Glick, I., and Bali, L. (1978). Prestimulus Effects on Human Startle Reflex in Normals and Schizophrenics. Psychophysiology *15*, 339–343.

Braff, D.L., Geyer, M.A., and Swerdlow, N.R. (2001). Human studies of prepulse inhibition of startle: normal subjects, patient groups, and pharmacological studies. Psychopharmacology (Berl.) *156*, 234–258.

Castellanos, F.X., Fine, E.J., Kaysen, D., Marsh, W.L., Rapoport, J.L., and Hallett, M. (1996). Sensorimotor gating in boys with Tourette's syndrome and ADHD: Preliminary results. Biol. Psychiatry *39*, 33–41.

Cedar, H., and Bergman, Y. (2009). Linking DNA methylation and histone modification: patterns and paradigms. Nat. Rev. Genet. *10*, 295–304.

Chen, E.S., Ernst, C., and Turecki, G. (2011). The epigenetic effects of antidepressant treatment on human prefrontal cortex BDNF expression. Int. J. Neuropsychopharmacol. *14*, 427–429.

Collins, B.E., Greer, C.B., Coleman, B.C., and Sweatt, J.D. (2019). Histone H3 lysine K4 methylation and its role in learning and memory. Epigenetics Chromatin *12*.

Conti, L.H. (2012). Interactions Between Corticotropin-Releasing Factor and the Serotonin 1A Receptor System on Acoustic Startle Amplitude and Prepulse Inhibition of the Startle Response in Two Rat Strains. Neuropharmacology *62*, 256–263.

Covington, H.E., Maze, I., LaPlant, Q.C., Vialou, V.F., Ohnishi, Y.N., Berton, O., Fass, D.M., Renthal, W., Rush, A.J., Wu, E.Y., et al. (2009). Antidepressant actions of histone deacetylase inhibitors. J. Neurosci. Off. J. Soc. Neurosci. *29*, 11451–11460.

Datko, M.C., Hu, J.-H., Williams, M., Reyes, C.M., Lominac, K.D., von Jonquieres, G., Klugmann, M., Worley, P.F., and Szumlinski, K.K. (2017). Behavioral and neurochemical phenotyping of mice incapable of homer1a induction. Front. Behav. Neurosci. *11*.

Davis, C.A., Hitz, B.C., Sloan, C.A., Chan, E.T., Davidson, J.M., Gabdank, I., Hilton, J.A., Jain, K., Baymuradov, U.K., Narayanan, A.K., et al. (2018). The Encyclopedia of DNA elements (ENCODE): data portal update. Nucleic Acids Res. *46*, D794–D801.

Dawson, M.A., and Kouzarides, T. (2012). Cancer epigenetics: from mechanism to therapy. Cell *150*, 12–27.

DeLisi, L.E., Razi, K., Stewart, J., Relja, M., Shields, G., Smith, A.B., Wellman, N., Larach, V.W., Loftus, J., Vita, A., et al. (2000). No evidence for a parent-of-origin effect detected in the pattern of inheritance of schizophrenia. Biol. Psychiatry *48*, 706–709.

Dietz, K.C., and Casaccia, P. (2010). HDAC inhibitors and neurodegeneration: at the edge between protection and damage. Pharmacol. Res. Off. J. Ital. Pharmacol. Soc. *62*, 11–17.

ENCODE Project Consortium (2012). An integrated encyclopedia of DNA elements in the human genome. Nature *489*, 57–74.

Fletcher, P.J., Rizos, Z., Noble, K., and Higgins, G.A. (2011). Impulsive action induced by amphetamine, cocaine and MK801 is reduced by 5-HT2C receptor stimulation and 5-HT2A receptor blockade. Neuropharmacology *61*, 468–477.

Fomsgaard, L., Moreno, J.L., de la Fuente Revenga, M., Brudek, T., Adamsen, D., Rio-Alamos, C., Saunders, J., Klein, A.B., Oliveras, I., Cañete, T., et al. (2018). Differences in 5-HT2A and mGlu2 Receptor Expression Levels and Repressive Epigenetic Modifications at the 5-HT2A Promoter Region in the Roman Low- (RLA-I) and High- (RHA-I) Avoidance Rat Strains. Mol. Neurobiol. *55*, 1998–2012.

Gandal, M.J., Haney, J.R., Parikshak, N.N., Leppa, V., Ramaswami, G., Hartl, C., Schork, A.J., Appadurai, V., Buil, A., Werge, T.M., et al. (2018). Shared molecular neuropathology across major psychiatric disorders parallels polygenic overlap. Science *359*, 693–697.

Geyer, M.A., and Swerdlow, N.R. (1998). Measurement of Startle Response, Prepulse Inhibition, and Habituation. Curr. Protoc. Neurosci. *3*, 8.7.1-8.7.15.

Gilpin, N.W., Richardson, H.N., Lumeng, L., and Koob, G.F. (2008). Dependence-Induced Alcohol Drinking by Alcohol-Preferring (P) Rats and Outbred Wistar Rats. Alcohol. Clin. Exp. Res. *32*, 1688–1696.

Giorgi, O., Piras, G., Lecca, D., Hansson, S., Driscoll, P., and Corda, M.G. (2003). Differential neurochemical properties of central serotonergic transmission in Roman high- and low-avoidance rats. J. Neurochem. *86*, 422–431.

González-Maeso, J., Ang, R.L., Yuen, T., Chan, P., Weisstaub, N.V., López-Giménez, J.F., Zhou, M., Okawa, Y., Callado, L.F., Milligan, G., et al. (2008). Identification of a serotonin/glutamate receptor complex implicated in psychosis. Nature *452*, 93–97.

Gottesman, I.I., and Carey, G. (1983). Extracting meaning and direction from twin data. Psychiatr. Dev. *1*, 35–50.

Graham, F.K. (1975). The More or Less Startling Effects of Weak Prestimulation. Psychophysiology *12*, 238–248.

Gratten, J., Wray, N.R., Keller, M.C., and Visscher, P.M. (2014). Large-scale genomics unveils the genetic architecture of psychiatric disorders. Nat. Neurosci. *17*, 782–790.

Grewal, S.I.S., and Moazed, D. (2003). Heterochromatin and Epigenetic Control of Gene Expression. Science *301*, 798–802.

Heintzman, N.D., Hon, G.C., Hawkins, R.D., Kheradpour, P., Stark, A., Harp, L.F., Ye, Z., Lee, L.K., Stuart, R.K., Ching, C.W., et al. (2009). Histone Modifications at Human Enhancers Reflect Global Cell Type-Specific Gene Expression. Nature *459*, 108–112.

Henikoff, S., and Shilatifard, A. (2011). Histone modification: cause or cog? Trends Genet. *27*, 389–396.

Holliday, R. (1994). Epigenetics: An overview. Dev. Genet. *15*, 453–457.

Hollis, F., Duclot, F., Gunjan, A., and Kabbaj, M. (2011). Individual differences in the effect of social defeat on anhedonia and histone acetylation in the rat hippocampus. Horm. Behav. *59*, 331–337.

Kendler, K.S., and Diehl, S.R. (1993). The Genetics of Schizophrenia: A Current, Genetic-epidemiologic Perspective. Schizophr. Bull. *19*, 261–285.

Kendler, K.S., and Robinette, C.D. (1983). Schizophrenia in the National Academy of Sciences-National Research Council Twin Registry: a 16-year update. Am. J. Psychiatry *140*, 1551–1563.

Kessler, S. (1980). The genetics of schizophrenia: a review. Schizophr. Bull. *6*, 404–416.

Klein, A.B., Ultved, L., Adamsen, D., Santini, M.A., Tobeña, A., Fernandez-Teruel, A., Flores, P., Moreno, M., Cardona, D., Knudsen, G.M., et al. (2014). 5-HT2A and mGlu2 receptor binding levels are related to differences in impulsive behavior in the Roman Low- (RLA) and High- (RHA) avoidance rat strains. Neuroscience *263*, 36–45.

Kouzarides, T. (2007). Chromatin Modifications and Their Function. Cell *128*, 693–705.

Kurita, M., Holloway, T., García-Bea, A., Kozlenkov, A., Friedman, A.K., Moreno, J.L., Heshmati, M., Golden, S.A., Kennedy, P.J., Takahashi, N., et al. (2012). HDAC2 regulates atypical antipsychotic responses through the modulation of mGlu2 promoter activity. Nat. Neurosci. *15*, 1245–1254.

Licht, J.D. (2015). DNA Methylation Inhibitors in Cancer Therapy: The Immunity Dimension. Cell *162*, 938–939.

Luger, K., Mäder, A.W., Richmond, R.K., Sargent, D.F., and Richmond, T.J. (1997). Crystal structure of the nucleosome core particle at 2.8 A resolution. Nature *389*, 251–260.

Mansbach, R.S., and Geyer, M.A. (1991). Parametric determinants in pre-stimulus modification of acoustic startle: Interaction with ketamine. Psychopharmacology (Berl.) *105*, 162–168.

Martinez, Z.A., Oostwegel, J., Geyer, M.A., Ellison, G.D., and Swerdlow, N.R. (2000). "Early" and "Late" Effects of Sustained Haloperidol on Apomorphine- and Phencyclidine-induced Sensorimotor Gating Deficits. Neuropsychopharmacology *23*, 517–527.

McAlonan, G.M. (2002). Brain anatomy and sensorimotor gating in Asperger's syndrome. Brain *125*, 1594–1606.

McCullough, S.D., On, D.M., and Bowers, E.C. (2017). Using Chromatin Immunoprecipitation in Toxicology: A Step-by-Step Guide to Increasing Efficiency, Reducing Variability, and Expanding Applications. Curr. Protoc. Toxicol. *72*, 3.14.1–3.14.28.

Mcghie, A., and Chapman, J. (1961). Disorders of attention and perception in early schizophrenia. Br. J. Med. Psychol. *34*, 103–116.

McInnis, M.G., McMahon, F.J., Crow, T., Ross, C.A., and DeLisi, L.E. (1999). Anticipation in schizophrenia: a review and reconsideration. Am. J. Med. Genet. *88*, 686–693.

Moreno, R., Sobotzik, J.-M., Schultz, C., and Schmitz, M.L. (2010). Specification of the NF-kappaB transcriptional response by p65 phosphorylation and TNF-induced nuclear translocation of IKK epsilon. Nucleic Acids Res. *38*, 6029–6044.

Nichols, J.R., and Hsiao, S. (1967). Addiction liability of albino rats: breeding for quantitive differences in morphine drinking. Science *157*, 561–563.

Oliveras, I., Rio-Alamos, C., Cañete, T., Blazquez, G., Martínez-Membrives, E., Giorgi, O., Corda, M.G., Tobeña, A., and Fernández-Teruel, A. (2015). Prepulse inhibition predicts spatial working memory performance in the inbred Roman high- and low-avoidance rats and in genetically heterogeneous NIH-HS rats: relevance for studying pre-attentive and cognitive anomalies in schizophrenia. Front. Behav. Neurosci. *9*, 213.

O'Neill, M.F., Heron-Maxwell, C.L., and Shaw, G. (1999). 5-HT2 receptor antagonism reduces hyperactivity induced by amphetamine, cocaine, and MK-801 but not D1 agonist C-APB. Pharmacol. Biochem. Behav. *63*, 237–243.

Østerbøg, T.B., On, D.M., Oliveras, I., Río-Álamos, C., Sanchez-Gonzalez, A., Tapias-Espinosa, C., Tobeña, A., González-Maeso, J., Fernández-Teruel, A., and Aznar, S. (2019). Metabotropic

Glutamate Receptor 2 and Dopamine Receptor 2 Gene Expression Predict Sensorimotor Gating Response in the Genetically Heterogeneous NIH-HS Rat Strain. Mol. Neurobiol.

Owens, S.F., Rijsdijk, F., Picchioni, M.M., Stahl, D., Nenadic, I., Murray, R.M., and Toulopoulou, T. (2011). Genetic overlap between schizophrenia and selective components of executive function. Schizophr. Res. *127*, 181–187.

Pchelintsev, N.A., Adams, P.D., and Nelson, D.M. (2016). Critical Parameters for Efficient Sonication and Improved Chromatin Immunoprecipitation of High Molecular Weight Proteins. PLOS ONE *11*, e0148023.

Penney, J., and Tsai, L.-H. (2014). Histone deacetylases in memory and cognition. Sci. Signal. *7*, re12.

Petronis, A., Gottesman, I.I., Crow, T.J., DeLisi, L.E., Klar, A.J., Macciardi, F., McInnis, M.G., McMahon, F.J., Paterson, A.D., Skuse, D., et al. (2000). Psychiatric epigenetics: a new focus for the new century. Mol. Psychiatry *5*, 342–346.

Pierce, R.C., Fant, B., Swinford-Jackson, S.E., Heller, E.A., Berrettini, W.H., and Wimmer, M.E. (2018). Environmental, genetic and epigenetic contributions to cocaine addiction. Neuropsychopharmacology *43*, 1471–1480.

Ponomarev, I., Wang, S., Zhang, L., Harris, R.A., and Mayfield, R.D. (2012). Gene Coexpression Networks in Human Brain Identify Epigenetic Modifications in Alcohol Dependence. J. Neurosci. *32*, 1884–1897.

Renthal, W., Maze, I., Krishnan, V., Covington, H.E., Xiao, G., Kumar, A., Russo, S.J., Graham, A., Tsankova, N., Kippin, T.E., et al. (2007). Histone Deacetylase 5 Epigenetically Controls Behavioral Adaptations to Chronic Emotional Stimuli. Neuron *56*, 517–529.

Renthal, W., Kumar, A., Xiao, G., Wilkinson, M., Covington, H.E., Maze, I., Sikder, D., Robison, A.J., LaPlant, Q., Dietz, D.M., et al. (2009). Genome-wide Analysis of Chromatin Regulation by Cocaine Reveals a Role for Sirtuins. Neuron *62*, 335–348.

Rodríguez-Ubreva, J., and Ballestar, E. (2014). Chromatin immunoprecipitation. Methods Mol. Biol. Clifton NJ *1094*, 309–318.

Rogge, G.A., and Wood, M.A. (2013). The Role of Histone Acetylation in Cocaine-Induced Neural Plasticity and Behavior. Neuropsychopharmacology *38*, 94–110.

Schreiber, S.L., and Bernstein, B.E. (2002). Signaling network model of chromatin. Cell *111*, 771–778.

Sipes, T.E., and Geyer, M.A. (1995). DOI disruption of prepulse inhibition of startle in the rat is mediated by 5-HT2A and not by 5-HT2C receptors. Behav. Pharmacol. *6*, 839–842.

Sproul, D., and Meehan, R.R. (2013). Genomic insights into cancer-associated aberrant CpG island hypermethylation. Brief. Funct. Genomics *12*, 174–190.

Stine, O.C., Xu, J., Koskela, R., McMahon, F.J., Gschwend, M., Friddle, C., Clark, C.D., McInnis, M.G., Simpson, S.G., Breschel, T.S., et al. (1995). Evidence for Linkage of Bipolar Disorder to Chromosome 18 with a Parent-of-Origin Effect. Am. J. Hum. Genet. *57*, 1384–1394.

Strahl, B.D., and Allis, C.D. (2000). The language of covalent histone modifications. Nature *403*, 41–45.

Swerdlow, N.R., and Geyer, M.A. (1993). Clozapine and haloperidol in an animal model of sensorimotor gating deficits in schizophrenia. Pharmacol. Biochem. Behav. *44*, 741–744.

Swerdlow, N.R., and Geyer, M.A. (1998). Using an animal model of deficient sensorimotor gating to study the pathophysiology and new treatments of schizophrenia. Schizophr. Bull. *24*, 285–301.

Swerdlow, N.R., Braff, D.L., Masten, V.L., and Geyer, M.A. (1990). Schizophrenic-like sensorimotor gating abnormalities in rats following dopamine infusion into the nucleus accumbens. Psychopharmacology (Berl.) *101*, 414–420.

Swerdlow, N.R., Benbow, C.H., Zisook, S., Geyer, M.A., and Braff, D.L. (1993). A preliminary assessment of sensorimotor gating in patients with obsessive compulsive disorder. Biol. Psychiatry *33*, 298–301.

Swerdlow, N.R., Paulsen, J., Braff, D.L., Butters, N., Geyer, M.A., and Swenson, M.R. (1995). Impaired prepulse inhibition of acoustic and tactile startle response in patients with Huntington's disease. J. Neurol. Neurosurg. Psychiatry *58*, 192–200.

Swerdlow, N.R., Talledo, J., Sutherland, A.N., Nagy, D., and Shoemaker, J.M. (2006). Antipsychotic Effects on Prepulse Inhibition in Normal 'Low Gating' Humans and Rats. Neuropsychopharmacology *31*, 2011–2021.

Swerdlow, N.R., Braff, D.L., and Geyer, M.A. (2016). Sensorimotor gating of the startle reflex: what we said 25 years ago, what has happened since then, and what comes next. J. Psychopharmacol. (Oxf.) *30*, 1072–1081.

Tan, M., Luo, H., Lee, S., Jin, F., Yang, J.S., Montellier, E., Buchou, T., Cheng, Z., Rousseaux, S., Rajagopal, N., et al. (2011). Identification of 67 Histone Marks and Histone Lysine Crotonylation as a New Type of Histone Modification. Cell *146*, 1016–1028.

Telford, D.J., and Stewart, B.W. (1989). Micrococcal nuclease: Its specificity and use for chromatin analysis. Int. J. Biochem. *21*, 127–138.

The US Burden of Disease Collaborators, Mokdad, A.H., Ballestros, K., Echko, M., Glenn, S., Olsen, H.E., Mullany, E., Lee, A., Khan, A.R., Ahmadi, A., et al. (2018). The State of US Health, 1990-2016: Burden of Diseases, Injuries, and Risk Factors Among US States. JAMA *319*, 1444.

Thorne, A.W., Myers, F.A., and Hebbes, T.R. (2004). Native chromatin immunoprecipitation. Methods Mol. Biol. Clifton NJ *287*, 21–44.

Trautmann, S., Rehm, J., and Wittchen, H. (2016). The economic costs of mental disorders: Do our societies react appropriately to the burden of mental disorders? EMBO Rep. *17*, 1245–1249.

Tsankova, N.M., Berton, O., Renthal, W., Kumar, A., Neve, R.L., and Nestler, E.J. (2006). Sustained hippocampal chromatin regulation in a mouse model of depression and antidepressant action. Nat. Neurosci. *9*, 519–525.

Valls-Solé, J., Muñoz, J.E., and Valldeoriola, F. (2004). Abnormalities of prepulse inhibition do not depend on blink reflex excitability: a study in Parkinson's disease and Huntington's disease. Clin. Neurophysiol. Off. J. Int. Fed. Clin. Neurophysiol. *115*, 1527–1536.

Volkow, N.D., Michaelides, M., and Baler, R. (2019). The Neuroscience of Drug Reward and Addiction. Physiol. Rev. *99*, 2115–2140.

Waddington, C.H. (1942). Canalization of Development and the Inheritance of Acquired Characters. Nature *150*, 563–565.

Wang, L., Xu, Z., Khawar, M.B., Liu, C., and Li, W. (2017). The histone codes for meiosis. Reproduction *154*, R65–R79.

Wang, Z., Zang, C., Rosenfeld, J.A., Schones, D.E., Barski, A., Cuddapah, S., Cui, K., Roh, T.-Y., Peng, W., Zhang, M.Q., et al. (2008). Combinatorial patterns of histone acetylations and methylations in the human genome. Nat. Genet. *40*, 897–903.

Wheeler, J.M., Reed, C., Burkhart-Kasch, S., Li, N., Cunningham, C.L., Janowsky, A., Franken, F.H., Wiren, K.M., Hashimoto, J.G., Scibelli, A.C., et al. (2009). Genetically correlated effects of selective breeding for high and low methamphetamine consumption. Genes Brain Behav. *8*, 758–771.

Wilkinson, M.B., Xiao, G., Kumar, A., LaPlant, Q., Renthal, W., Sikder, D., Kodadek, T.J., and Nestler, E.J. (2009). Imipramine Treatment and Resiliency Exhibit Similar Chromatin Regulation in the Mouse Nucleus Accumbens in Depression Models. J. Neurosci. *29*, 7820–7832.

Wischhof, L., Hollensteiner, K., and Koch, M. (2011). Impulsive behaviour in rats induced by intracortical DOI infusions is antagonized by co-administration of an mGlu2/3 receptor agonist. Behav. Pharmacol. *22*, 805–813.

Zebardast, N., Crowley, M.J., Bloch, M.H., Mayes, L.C., Wyk, B.V., Leckman, J.F., Pelphrey, K.A., and Swain, J.E. (2013). Brain mechanisms for prepulse inhibition in adults with Tourette syndrome: Initial findings. Psychiatry Res. Neuroimaging *214*, 33–41.